AALTO UNIVERSITY
SCHOOL OF ELECTRICAL ENGINEERING
Department of communications and Networking (Comnet)

Yihenew Dagne Beyene

TV Black-space Spectrum Access for Wireless Local Area and Cellular Networks

A thesis submitted in partial fulfillment of the requirements for the degree of Master of Science in Technology.

Helsinki, August 10, 2012

Supervisor: Riku Jäntti, Professor, D.Sc

Instructor: Kalle Ruttik, D.Sc

AALTO UNIVERSITY
SCHOOL OF ELECTRICAL ENGINEERING

ABSTRACT OF THE
MASTER'S THESIS

Author:	Yihenew Dagne Beyene
Name of the Thesis:	TV Black-space Spectrum Access for Wireless Local Area and Cellular Networks
Date:	August 10, 2012 **Number of pages:** 72
Department:	Department of Communications and Networking
Professorship:	S-72
Supervisor:	Riku Jäntti, Professor, D.Sc
Instructor:	Kalle Ruttik, D.Sc

This thesis presents a black-space spectrum access scheme for overlay cognitive radio in TV band. Physical layer implementations of secondary systems using software defined radio technology have been proposed. We consider two types of secondary transmitters with WLAN-type and LTE-type frame structures in order to study the impact of secondary transmission over primary pilot carriers on performances of channel estimation and interference cancellation algorithms. Bit error rate has been used as performance metric, and performances of the two secondary systems have been presented in different scenarios. The effect of secondary transmitters interference power level on performances of primary and secondary receivers has been investigated.

Keywords: Cognitive radio, overlay, Interference channel, GNU Radio, DVB, WLAN, LTE

Acknowledgements

This thesis is part of *End-to-End Cognitive Radio Testbed* (EECRT) project at Department of Communications and Networking, Aalto University. I would like to thank my supervisor, professor Riku Jäntti, for giving me the chance to work in this project. Moreover, I owe my gratitude to my instructor, Dr. Kalle Ruttik, for his invaluable advices and comments throughout the course of my work. I also acknowledge Viktor Nässi who gave me technical supports during my stay at communications laboratory.

I greatly appreciate Juha Vierinen and Lassi Roininen, researchers at Sodankylä Geophysical Observatory, for recommending me to study in Finland which is known for its leading-edge research in telecommunications engineering.

Finally, thanks to all who deserve gratitude and blessings in more than words.

Otaniemi, August 10, 2012

Yihenew Dagne Beyene

Contents

List of Abbreviations vii

List of Notations x

List of Figures xv

List of Tables xvi

1 Introduction 1

1.1 Cognitive radio . . . 2

1.2 Scope of the thesis . . . 2

1.3 Thesis organization . . . 3

2 OFDMA Systems 4

2.1 OFDM principles . . . 4

2.2 OFDM in wireless channels . . . 9

2.3 DVB system . . . 11

2.4 IEEE 802.11-2007 OFDM physical layer . . . 14

2.5 LTE physical layer (Release 8) . . . 16

3 Cognitive Radios - Interference Channels 20

3.1 Secondary spectrum access . . . 20

3.1.1 Interweave system . . . 21

3.1.2 Underlay system . . . 22

3.1.3 Overlay system . . . 23

3.2 Interference channel 23
3.3 Orthogonal channel access 26
3.4 General Gaussian interference channel 26

4 Overlay Cognitive Radio **31**
4.1 Overlay cognitive radio Gaussian channel 32
4.2 Achievable capacity 34
4.3 Practical considerations 37
4.4 Overlay transmitter 40
4.5 Overlay receiver 42

5 Implementation **48**
5.1 Implementation platform 48
5.1.1 GNU Radio and USRP 49
5.2 WLAN-type overlay transmitter 49
5.2.1 Packet encoder and scrambler 51
5.2.2 OFDM mapper 51
5.2.3 Insert preamble 51
5.2.4 IFFT 52
5.2.5 Cyclic prefix adder 52
5.2.6 Gain 52
5.2.7 USRP 52
5.3 WLAN-type overlay receiver 52
5.3.1 USRP 52
5.3.2 Channel filter 53
5.3.3 Synchronizer 53
5.3.4 Sampler 53
5.3.5 FFT 54
5.3.6 DVB equalizer 54
5.3.7 DVB demodulator 54
5.3.8 Frame acquisition 54
5.3.9 WLAN demodulator 55

5.3.10 Message decoder and descrambler 55
5.4 LTE-type overlay transmitter 55
5.4.1 Scrambler 56
5.4.2 Modulation mapper 56
5.4.3 Layer mapper 56
5.4.4 Precoder 57
5.4.5 Resource element mapper 57
5.4.6 Insert reference signals 57
5.4.7 IFFT 57
5.4.8 USRP 58
5.5 LTE overlay receiver 58
5.5.1 FD-sync 58
5.5.2 Equalizer 59
5.5.3 LTE demodulator 59
5.5.4 Message decoder 59

6 Results and Discussion **60**
6.1 Hardware characteristics 60
6.2 Measurement setup 60
6.3 Results 62

7 Conclusion **67**

List of Abbreviations

AGC	Automatic Gain Control
AWGN	Additive White Gaussian Noise
BER	Bit-Error-Rate
BW	BandWidth
CRC	Cyclic Redundancy Check
DL	DownLink
DSSS	Direct Sequence Spread Spectrum
DVB	Digital Video Broadcast
DVB-T	DVB-Terrestrial
DVB-H	DVB-Handheld
FCC	Federal Communications Commission
FDD	Frequency Division Duplexing
FDMA	Frequency Division Multiple Access
ICI	Inter-Carrier Interference
IDFT	Inverse Discrete Fourier Transform
IFFT	Inverse Fast Fourier Transform
IFO	Integer Frequency Offset

IR	InfraRed
ISI	Inter-Symbol Interference
ISM	Industrial, Scientific and Medical
LNA	Low Noise Amplifier
LS	Least Squares
LTE	Long Term Evolution
MAC	Medium Access Control
MIMO	Multiple-Input-Multiple-Output
MPDU	MAC Protocol Data Unit
MMSE	Minimum Mean-Square Error
MSE	Mean-Square Error
OFDM	Orthogonal Frequency Division Multiplexing
OFDMA	Orthogonal Frequency Division Multiple Access
PLCP	Physical Layer Convergence Procedure
PMD	Physical Medium Dependent
PLME	Physical Layer Management Entity
PPDU	PLCP Protocol Data Unit
PRBS	Pseudo-Random Binary Sequence
PSDU	PLCP Service Data Unit
RMS	Root-Mean-Square
SDR	Software Defined Radio
SINR	Signal-to-Interference-Noise Ratio

SIR	Signal-to-Interference Ratio
SNR	Signal-to-Noise Ratio
TDD	Time Division Duplexing
TDMA	Time Division Multiple Access
TPS	Transmission Parameter Signalling
TU	Typical Urban
UL	UpLink
UHD	Universal Hardware Driver
USB	Universal Serial Bus
USRP	Universal Software Radio Peripheral
WLAN	Wireless Local Area Network
ZF	Zero-Forcing

List of Notations

a_k	modulating complex symbol
a_n	Amplitude response of n^{th} multipath component
a_{ij}	Magnitude-square of c_{ij}
c_{ij}	Standard form transformation of h_{ij}
C	Channel capacity
C_{causal}	Channel capacity for causally known interference
g, G	Amplifier gain
h_{ij}	Channel gain between i^{th} transmitter and j^{th} receiver
$h(t)$	Instantaneous time-domain channel response
$h(t, \tau)$	Multipath channel response at time t for impulse transmitted at time $t - \tau$
$Im\{.\}$	Imaginary part
k_f	Frequency-dependent constant
$\mathcal{M}$	Transmitted message
P	Signal power
P_{τ_n}	Normalized power of n^{th} multipath component
$p_{m,I,k}$	Pilot signal on k^{th} subcarrier of I^{th} symbol in m^{th} DVB frame

Q	Average power of known Gaussian interference signal
R	Transmission rate over a channel
$Re\{.\}$	Real part
S	Known Gaussian interference signal
T_U	Useful time duration of OFDM symbol
T_S	Total OFDM symbol duration
w_k	k^{th} value in PRBS sequence
$x(t)$	Continuous-time signal
$X(f)$	Fourier-transform of $x(t)$
$x_T(t)$	Time-domain rectangular signal of duration T
$X_T(f)$	Fourier transform of $x_T(t)$
X	Channel input signal
$\mathcal{X}$	Channel input message alphabet set
X_c	Cognitive transmitter's own signal
X_p	Primary transmitted signal
X_s	Secondary transmitted signal
Y	Channel output signal
$\mathcal{Y}$	Channel output message alphabet sets
Z	Gaussian noise

γ	Signal-to-Interference Ratio
Δ	OFDM guard interval
$\Delta\tau(t)$	Excess delay
Δf	Inter-carrier spacing
$\bar{\tau}$	Weighted first moment of channel delay
$\bar{\tau^2}$	Weighted second moment of channel delay
τ_n	Time delay caused by n^{th} multipath component
τ_{rms}	RMS delay spread
ϕ_n	Phase response of n^{th} multipath component

List of Figures

2.1 Time-domain representation of a single subcarrier. T is the symbol duration. 5

2.2 Frequency spectrum of a single subcarrier (*sinc* function). T is the symbol duration in time domain. 5

2.3 Orthogonal multiplexing of subcarriers. At the peak of each subcarrier, interference from other sub-carriers is zero. 6

2.4 General block diagram of OFDM signal generation using IDFT. 7

2.5 ISI-free sampling of OFDM signal in multipath channel. 9

2.6 Illustration of multipath propagation. 10

2.7 Normalized channel power delay profile and magnitude response for TU. 11

2.8 Functional block diagram of DVB transmitter [1]. 12

2.9 PPDU frame structure of OFDM physical layer [2]. 15

2.10 Block diagram of uplink physical channel processing. 17

2.11 Block diagram of downlink physical channel processing. 17

2.12 LTE frame structure (type-1). 17

2.13 Time-frequency resource grid structure of LTE for normal cyclic prefix configuration. In multi-antenna transmission, each antenna port has one resource grid. 18

3.1 Interweave cognitive radio operation - secondary spectrum access on *white spaces*. 22

3.2 Underlay cognitive radio - secondary signal is spread over wide band with low power constrained by interference level tolerated by other non-cognitive users. 22

3.3 Overlay cognitive radio - secondary signal is added on top of the primary signal at relatively low power such that SNR requirement of the primary users is satisfied. 23

3.4 Interference channel with two inputs and two outputs. 24

3.5 Sequential decoding schemes of Gaussian interference channel. 27

3.6 Bounds for achievable rate regions for general Gaussian interference channel: (a) $P_1' = P_2' = 6$, $a_{12} = a_{21} = 0.1$, (b) $P_1' = P_2' = 6$, $a_{12} = a_{21} = 0.55$, (c) $P_1' = P_2' = 6$, $a_{12} = a_{21} = 5$ (d) $P_1' = P_2' = 6$, $a_{12} = a_{21} = 7$. 29

4.1 Concurrent operation of secondary system (cognitive) within the coverage area of primary system. 32

4.2 A two-input-two-output Gaussian interference channel with the second transmitter having non-causal messages of the primary. 33

4.3 Dirty-paper coding with additive Gaussian noise and Gaussian distributed interference, S, known by the transmitter. Power of the transmitted signal, $X = U - \alpha S$, is constrained by $(1/n)\sum_{i=1}^{n} X_i^2 \leq P$. 35

4.4 Illustration of DVB signal pilot structure. Unlike *scattered pilots*, *continual pilots* have fixed locations. 39

4.5 Proposed WLAN-type frame structure for *orthogonal pilot* overlay cognitive radio. 40

4.6 LTE-type frame structure with synchronization symbols and reference pilots. 41

4.7 Overlay transmitter design where $\mathcal{W}_p$ is the primary message encoded to X_p, and $\mathcal{W}_s$ is the secondary message encoded to X_c. The scaling factors, g and G, are calculated based on the power constraints, P_p and P_s, and relaying fraction, α^*, obtained in Equation (4.6). 41

4.8 Sequential decoding of secondary message. The equalizer estimates the channel using pilots of the primary signal. 42

4.9 Time-domain interpolation using (a) zero-order and (b) first-order polynomial filters [3]. 46

5.1 Software define radio. 48

5.2 Interaction among USRP hardware, GNU Radio and upper layers. 50

5.3 WLAN-type OFDM transmitter implementation using GNU Radio platform. 50

5.4 GNU Radio implementation of WLAN-type overlay receiver. . 53

5.5 GNU Radio implementation of LTE DL overlay transmitter. . 56

5.6 GNU Radio implementation of LTE-type overlay receiver. . . . 58

6.1 Measured BER for primary and secondary signals, $\gamma_p = 7dB$. . 63

6.2 Measured BER for primary and secondary signals, $\gamma_p = 12dB$. 65

6.3 Measured BER for primary and secondary signals, $\gamma_p = 17dB$. 66

List of Tables

2.1 Constellation points for uniform and non-uniform modulations in DVB [1]. 13

2.2 Comparison of OFDM parameters of DVB-T, WLAN and LTE physical layers. The parameter l is symbol number in an LTE time slot. 19

6.1 RF characteristics of hardware used during measurement. . . . 61

Chapter 1

Introduction

The radio spectrum is, nowadays, a scarce resource. On the other hand, not all licensed frequency bands are fully utilized. The spectrum has been divided into segments by the regulatory bodies such as FCC (Federal Communications Commission) of United States. These spectral segments are assigned for different kinds of wireless services such as radio and TV broadcasts, cellular networks, satellite communication, and others. Each frequency band segment is then divided into many channels which are granted to operators and other commercial and governmental institutions. This fixed allocation of resources ensures that there will be no interference between licensed users. However, it causes inefficient usage of the resources as some frequency bands may be highly occupied while there is little or no transmission on other bands. Underutilization of the radio resource can be in spatial, spectral and/or temporal domain.

The fact that demand for wireless traffic is increasing exponentially while there is limited radio resource suitable for wireless communication has been a driving force for researchers to come up with efficient modulation and coding schemes, protocols and multiple antenna diversity and multiplexing techniques. Optimization of radio access technologies was the main focus in this research. On the other hand, some radio spectra such as TV channels have been found to be inefficiently utilized [4]. Therefore, secondary networks can be deployed in such bands to access unused radio resources whenever available. Such oppor-

tunistic spectrum access requires reconfigurable radio system architecture.

1.1 Cognitive radio

Cognitive radio is a candidate technology that enables coexistence of multiple networks operating in the same frequency band. The concept was originally introduced by J. Mitola [5], and it has been defined in various ways since then [6], [7], [8]. In general, it is a radio system having some form of intelligence. The intelligence can be ability to sense signal spectrum and use this information to decide how and when to transmit over the given band. Unlike ordinary radios, cognitive radio has the capability of adapting to changes in its environment by changing its parameters such as modulation and coding schemes, frequency and power.

Cognitive radio can be employed to increase efficiency of utilization of the radio spectrum by allowing flexible sharing of the resource among multiple users without interfering each other. Realizing such system demands sophisticated signal processing by the cognitive transmitters and receivers in a way that maximal usage of the resource is achieved while making sure that other users will not suffer from interference caused by the cognitive transmitter. Reconfigurable signal processing needs of cognitive radios can be enabled via software defined radio (SDR) [9], [10] technology using high-speed programmable digital hardware and general purpose computers available today. In chapter 5 we will discuss more on practical implementation of overlay cognitive radio on an open-source software defined radio platform [11].

1.2 Scope of the thesis

Research in cognitive radio systems has received a lot of attention due to spectrum scarcity, and many articles on the topic have been published in recent days [8], [7], [12], [13]. Many of them are, however, based on a set of assumptions such as perfect knowledge of channel coefficients which might not exist in practical wireless communication systems. The thesis focuses

on a particular class of cognitive radio, specifically overlay cognitive radio. We will look into *black-space spectrum*[1] access scheme in DVB (Digital Video Broadcast) channels. We study how the quality of pilot symbols impacts secondary system's performance. Practical implementation of overlay system using LTE (Long Term Evolution) type and WLAN (Wireless Local Area Network) type frame structures using a software defined radio platform, and performance measurements results are presented.

1.3 Thesis organization

The thesis starts with defining fundamental concepts and mathematical models. Later practical implementation of overlay secondary sharing algorithm and discussion of measurement results are presented. Chapter 2 gives overview of OFDM (Orthogonal Frequency Division Multiplexing) modulation scheme which is used in latest radio access technologies. The chapter also briefly points out physical layer structures of targeted OFDMA systems, DVB, LTE and WLAN, in practical implementation. Chapter 3 introduces secondary spectrum access methods for cognitive radios. Chapter 4 discusses overlay cognitive radio channel and coexistence requirements for the cognitive radio. Later cognitive transmitter and receiver designs are presented. Chapter 5 focuses on practical realization of overlay cognitive radio on an open-source software defined radio platform. Measurement results of the system performance have been discussed in Chapter 6. Finally, Chapter 7 concludes the main observations on practical performance results and limitations of the system.

[1]It refers to an already occupied channel as seen by another secondary transmitter [7].

Chapter 2

OFDMA Systems

Orthogonal Frequency Division Multiplexing (OFDM) is a multi-carrier modulation scheme where a set of narrow-band orthogonal subcarriers are used to carry information. Due to its high spectral efficiency it has been adopted in latest cellular and local area networks. The transmitted signal is cyclically extended in time such that multipath components in fast fading environment can be combined without causing ISI (Inter-Symbol Interference).

The overlay cognitive radio implementation targets two OFDMA based cellular and WLAN systems as secondary transmitters in DVB (Digital Video Broadcast) channels. In this chapter, basics of OFDM and its advantage in fading environments will be discussed. Later, the physical layer structures of DVB, LTE and WLAN systems will be briefly presented.

2.1 OFDM principles

In OFDM, the data stream is converted into low-rate parallel streams each modulating a subcarrier. In frequency domain, the subcarriers are *sinc* waveforms which are rectangular pulses in time-domain. Figure 2.1 shows time domain representation of one subcarrier.

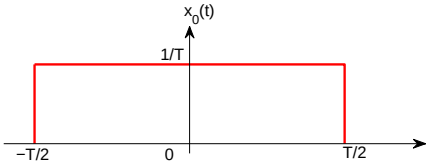

Figure 2.1: Time-domain representation of a single subcarrier. T is the symbol duration.

$$x_T(t) = \frac{1}{T}\text{rect}\left(\frac{t}{T}\right) \tag{2.1}$$

$$= \begin{cases} \frac{1}{T}, & \frac{-T}{2} \leq t < \frac{T}{2} \\ 0, & \text{elsewhere} \end{cases} \tag{2.2}$$

The frequency domain representation of the subcarrier is shown in Figure 2.2.

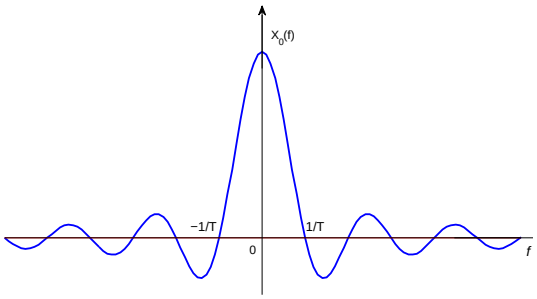

Figure 2.2: Frequency spectrum of a single subcarrier (*sinc* function). T is the symbol duration in time domain.

$$X_T(f) = sinc(fT) \tag{2.3}$$

Such sub-carriers are put aside to each other orthogonally while spectral overlap can be allowed. The orthogonality is maintained by centering each subcarrier at frequencies where other subcarriers have zero spectral component. In other words, we put them at intervals of $1/T$ Hz.

In OFDM, each subcarrier carries one modulating symbol (complex number)

so that one sample from each subcarrier is sufficient to recover the transmitted information. Orthogonality of carriers makes sure that there will be no interference from neighboring subcarriers at the instant of sampling as shown in Figure 2.3. The subcarrier spacing, Δf, is inversely proportional to the symbol period, T.

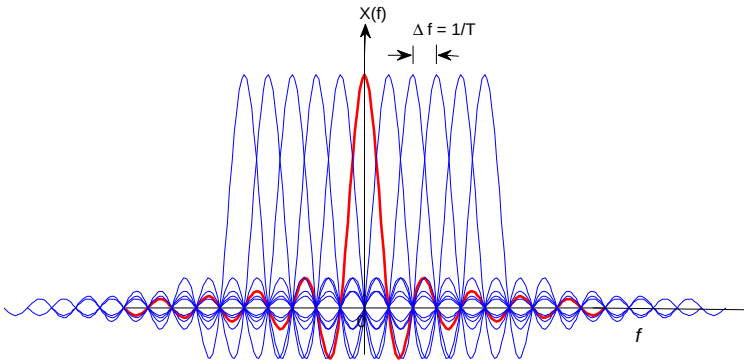

Figure 2.3: Orthogonal multiplexing of subcarriers. At the peak of each sub-carrier, interference from other sub-carriers is zero.

$$X(f) = \sum_{k=-M}^{M} X_T \left(f - \frac{k}{T} \right) \tag{2.4}$$

In general, each subcarrier, X_k, is modulated by a complex symbol, a_k, so that the baseband signal spectrum can be written as

$$X(f) = \sum_{k=-M}^{M} a_k X_T \left(f - \frac{k}{T} \right) \tag{2.5}$$

The corresponding time-domain signal will be

$$x(t) \quad = \quad \frac{1}{T} \sum_{k=-M}^{M} a_k e^{j2\pi k \frac{t}{T}} \, \mathsf{rect} \left(\frac{t}{T} \right) \tag{2.6}$$

The signal is bounded by finite time duration of T seconds. For time interval

$t \in [-T/2,\ T/2]$, $x(t)$ can be expressed as

$$x(t) = \frac{1}{T} \sum_{k=-M}^{M} a_k e^{j2\pi k \frac{t}{T}} \tag{2.7}$$

The orthogonal subcarriers are uniquely defined by the complex symbols, a_k, $k \in \{-M, -M+1, \cdots, M\}$. This implies that finite time-domain samples are sufficient for describing the signal. The minimum number of samples is equal to the number of subcarriers (or number of complex symbols) which is equal to $2M+1$. If we divide the symbol duration, T into $2M+1$ equally spaced bins ($T/(2M+1)$) we get discrete samples as sampling rate of $(2M+1)/T$ samples/second. This conforms to the Nyquist criterion.

The discrete-time version of the signal is

$$x[n] = x(nT/(2M+1)) \tag{2.8}$$

$$= \frac{1}{T} \sum_{k=-M}^{M} a_k e^{j2\pi nk/(2M+1)} \tag{2.9}$$

where $x[n]$ is the n^{th} discrete sample taken at $t = nT/(2M+1)$ seconds, $n \in \{0,\ 1, \cdots, 2M\}$.

The signal $x[n]$ is equivalent to Inverse Discrete Fourier Transform (IDFT) of the complex symbols, a_k. Therefore, OFDM can easily implemented as IDFT operation on the modulating complex symbols. Figure 2.4 shows IDFT implementation of OFDM signal.

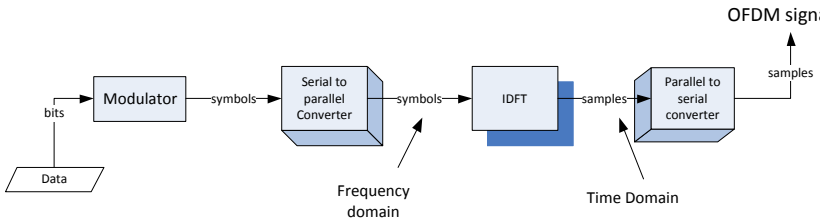

Figure 2.4: General block diagram of OFDM signal generation using IDFT.

Cyclic prefix

It can be seen that the time-domain OFDM signal, $x[n]$, is periodic. There are $2M+1$ samples in one period.

$$x[n-(2M+1)] = \frac{1}{T}\sum_{k=-M}^{M} a_k e^{j2\pi k\left(\frac{n}{2M+1}-1\right)} \tag{2.10}$$

$$= \frac{1}{T}\sum_{k=-M}^{M} e^{-j2\pi k} a_k e^{j2\pi nk/(2M+1)} \tag{2.11}$$

$$= \frac{1}{T}\sum_{k=-M}^{M} a_k e^{j2\pi nk/(2M+1)} \tag{2.12}$$

$$x[n-(2M+1)] = x[n] \tag{2.13}$$

Therefore, we can extend symbol duration to the left and right of the minimum duration, $[-M, -M+1, \cdots, M]$. Let us add one sample at $n = -M-1$. From the property of periodicity, we have

$$x[-M-1] = x[-M-1+(2M+1)] = x[M] \tag{2.14}$$

In general,

$$x[-M-l] = x[M+1-l], \qquad l = 1, 2, \cdots, L \tag{2.15}$$

The symbol duration is extended to the left by L samples taken from the last L samples of the interval $\{-M, -M+1, \cdots, M\}$. The cyclically added group of L extra samples is called *cyclic prefix*. From the extended symbol duration, $\{-M-L, -M-L+1, \cdots, M\}$, any $2M+1$ consecutive samples can be used to describe the signal. Different time shifts, however, will cause phase offset in frequency domain. The advantage of added cyclic prefix is to combine different multipath components of the received signal without causing ISI as shown in Figure 2.5. However, this is achieved at the cost of extra guard period which is not used to transmit information.

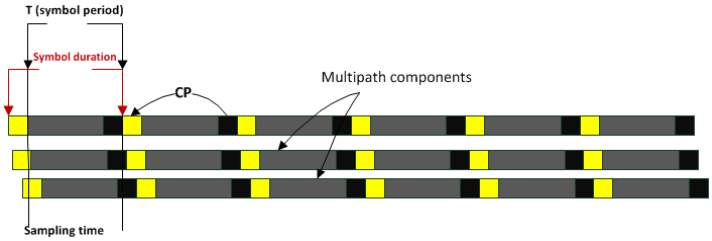

Figure 2.5: ISI-free sampling of OFDM signal in multipath channel.

2.2 OFDM in wireless channels

In wireless communication, electromagnetic waves propagate from the transmitter antenna to receiver antenna through air. Due to spreading of signal energy to wider area as it travels far away from the transmitter, the signal strength is attenuated exponentially. A simple free-space channel model is expressed as

$$h(t) = k_f \left(\frac{1}{d}\right)^2 \tag{2.16}$$

where $h(t)$ is the instantaneous (at time t) channel gain at a distance d, and k_f is a frequency-dependent constant.

In practical wireless communications, the communication channel is far from free space. Signal propagation is also affected by antenna type, antenna height and obstacles [14]. Moreover, the received signal is superposition of various signals arriving at different time instants from different directions. The signal from each path is a duplicate of the transmitted signal being distorted in amplitude, frequency and phase.
As shown in Figure 2.6 the transmitted signal is reflected from the surrounding objects before reaching at the receiver. The reflection and diffraction effects cause phase shift on the signal. The phase shift is time-variant if there is mobility in the transmitter, reflectors, and/or receiver. A finite multipath component approximation of the channel is given by [3]

$$h(\tau, t) = \sum_{n=1}^{N} a_n(t) e^{j\phi_n(t)} \delta(\tau - \tau_n(t)) \tag{2.17}$$

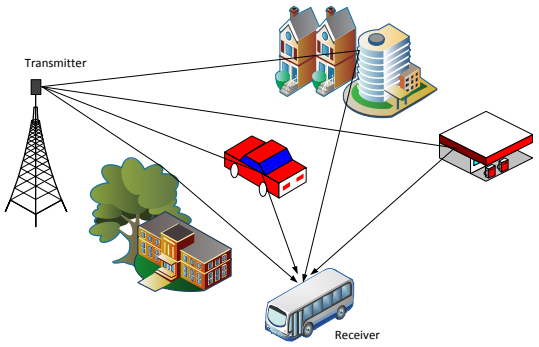

Figure 2.6: Illustration of multipath propagation.

where $h(t,\tau)$ is the channel response at time t for the impulse transmitted at time $t-\tau$, and a_n, ϕ_n, τ_n are time-varying amplitude response, phase shift and time delay caused by the n^{th} path. The excess delay $\Delta\tau(t)$ is defined as time difference between the first and the last arriving multipath components.

Root-mean-square (RMS) delay spread

RMS delay spread is defined as weighted RMS delay given by Equation 2.18. It is expressed as

$$\tau_{rms} = \sqrt{\bar{\tau^2} - (\bar{\tau})^2} \tag{2.18}$$

where $\bar{\tau}$ and $\bar{\tau^2}$ are weighted first and second moments of delays. The weights are normalized powers of multipath components [3]. Normalized power of n^{th} multipath component given by

$$p_{\tau_n} = \frac{E\left\{|a_n(t)|^2\right\}}{\sum_{n=1}^{N} E\left\{|a_n(t)|^2\right\}} \tag{2.19}$$

The RMS delay spread, hence, takes the form

$$\tau_{rms} = \sqrt{\sum_{n=1}^{N} \left(\tau_n - \sum_{n=1}^{N} \tau_n p_{\tau_n}\right)^2 p_{\tau_n}} \tag{2.20}$$

where

$$\sum_{n=1}^{N} p_{\tau_n} = 1 \tag{2.21}$$

RMS delay spread is a measure of frequency selectivity of the channel. A value larger than the symbol duration, causes Inter Symbol Interference (ISI). Equivalently, the channel's frequency response is not flat over the signal bandwidth. For communication systems with symbol duration smaller than the RMS delay spread, the channel is said to be frequency-selective; otherwise, it is called frequency-flat channel. In practical systems, the symbol duration is made sufficiently large. Figure 2.7 shows channel impulse response and frequency response for a typical urban (TU) channel model [15]. The RMS delay spread in this model is $0.5\mu s$. In LTE downlink, the typical symbol duration

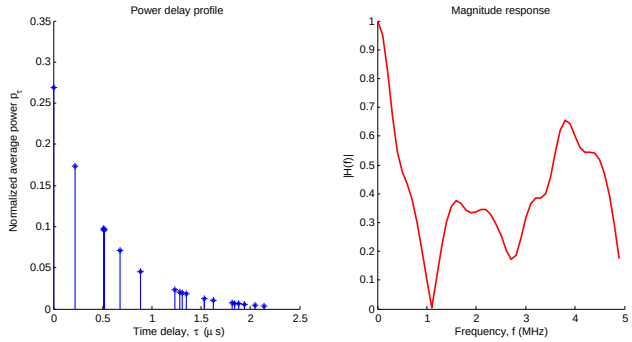

Figure 2.7: Normalized channel power delay profile and magnitude response for TU.

is $66.7\mu s$ for type-1 frame structure [16]. The shortest cyclic prefix duration is $4.7\mu s$ which is much larger than the channel delay spread. Therefore, multipath components can be effectively combined without causing ISI.

2.3 DVB system

The physical layer standard for digital terrestrial broadcast system defines OFDM based frame structure of the baseline transmitter [1]. The OFDM system is specified for 6 MHz, 7 MHz and 8 MHz channels. While the same specification applies to these options in frame structure, the sample rate varies

accordingly. Hierarcheal modulation and coding are used to multiplex two MPEG transport streams using uniform and multi-resolution constellation. Figure 2.8 shows functional block diagram of the transmitter. The receiver uses the same set of decoders and de-interleavers for each stream.

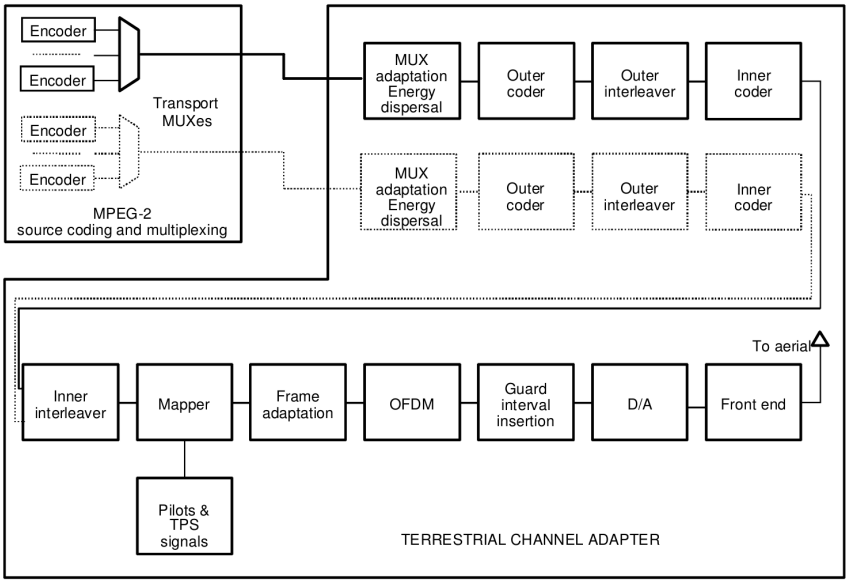

Figure 2.8: Functional block diagram of DVB transmitter [1].

DVB frame structure

One OFDM frame comprises 68 OFDM symbols each with duration $T_S = T_U + \Delta$ where T_U is the useful part, and Δ is the guard interval. Four guard interval values are defined: $\Delta/T_U = 1/4, 1/8, 1/16, 1/32$. Two transmission modes, "2K mode" and "8K mode", are available for DVB-T (DVB-Terrestrial) and DVB-H (DVB-Handheld) systems where an OFDM symbols contains 6817 carriers in the 8K mode and 1705 carriers in 2K mode. Each carrier is assigned to either data symbols, *scattered* pilots, *continual* pilots or TPS (Transmission Parameter Signalling) pilots.

One MPEG-2 transport multiplex packet containing 188 bytes is mapped to each OFDM symbol. All data carriers in one OFDM frame are modulated using either QPSK, 16-QAM, 64-QAM, non-uniform 16-QAM or non-uniform

Modulation	Normalized constellations: $n + jm$
QPSK	$n, m \in \{-\frac{1}{\sqrt{2}}, \frac{1}{\sqrt{2}}\}$
16-QAM (non-hierarchical and hierarchical with $\alpha = 1$)	$n, m \in \{-\frac{3}{\sqrt{10}}, -\frac{1}{\sqrt{10}}, \frac{1}{\sqrt{10}}, \frac{3}{\sqrt{10}}\}$
Non-uniform 16-QAM with $\alpha = 2$	$n, m \in \{-\frac{4}{\sqrt{20}}, -\frac{2}{\sqrt{20}}, \frac{2}{\sqrt{20}}, \frac{4}{\sqrt{20}}\}$
Non-uniform 16-QAM with $\alpha = 4$	$n, m \in \{-\frac{6}{\sqrt{52}}, \frac{4}{\sqrt{52}}, \frac{4}{\sqrt{52}}, \frac{6}{\sqrt{52}}\}$
64-QAM (non-hierarchical and hierachical with $\alpha = 1$)	$n, m \in \{-\frac{7}{\sqrt{42}}, -\frac{5}{\sqrt{42}}, -\frac{3}{\sqrt{42}}, -\frac{1}{\sqrt{42}}, \frac{1}{\sqrt{42}}, \frac{3}{\sqrt{42}}, \frac{5}{\sqrt{42}}, \frac{7}{\sqrt{42}}\}$
Non-uniform 64-QAM with $\alpha = 2$	$n, m \in \{-\frac{8}{\sqrt{60}}, -\frac{6}{\sqrt{60}}, -\frac{4}{\sqrt{60}}, -\frac{2}{\sqrt{60}}, \frac{2}{\sqrt{60}}, \frac{4}{\sqrt{60}}, \frac{6}{\sqrt{60}}, \frac{8}{\sqrt{60}}\}$
Non-uniform 64-QAM with $\alpha = 4$	$n, m \in \{-\frac{10}{\sqrt{108}}, -\frac{8}{\sqrt{108}}, -\frac{6}{\sqrt{108}}, -\frac{4}{\sqrt{108}}, \frac{4}{\sqrt{108}}, \frac{6}{\sqrt{108}}, \frac{8}{\sqrt{108}}, \frac{10}{\sqrt{108}}\}$

Table 2.1: Constellation points for uniform and non-uniform modulations in DVB [1].

64-QAM. Non-uniform constellation apply only for hierarchical transmission. Table 2.1 shows constellation points for different modulation schemes in DVB. The parameter α is the ratio of the minimum distance separating two constellation points having different high priority bit stream values and the minimum distance between any two constellation points [1].

Subcarriers (*cells*) containing reference signals (*scattered* pilots and *continual* pilots) are transmitted at boosted power levels. The pilot information is derived from a Pseudo-Random Binary Sequence (PRBS). The locations of scattered pilots changes from one symbol to another. On the other hand, *continual* pilots have fixed locations, and there are 45 *continual* pilots in 2K mode and 177 in 8K mode. The modulation value of *continual* and *scattered* pilots is a complex number, $p_{m,I,k}$, given by

$$Re\{p_{m,I,k}\} = 4/3 \cdot 2(1/2 - w_k) \quad (2.22)$$

$$Im\{p_{m,I,k}\} = 0 \quad (2.23)$$

where m is the frame index, k is the subcarrier index, I is the symbol index and w_k is a PRBS sequence generated by a polynomial $x^{11} + x^2 + 1$.

TPS carriers are used for signaling transmission information: modulation, hierarchy, guard interval, code rate, transmission mode, frame number and cell identification. The same TPS information is transmitted on 17 carriers (2K mode) and 68 carriers (8K mode) in every OFDM symbol.

2.4 IEEE 802.11-2007 OFDM physical layer

IEEE 802.11 is a standard for wireless local area networks (WLANs) that defines physical layer and MAC layer functions. It is the most widely deployed wireless access technology worldwide. Different types of physical layers are defined to work with the same MAC layer protocol. The physical layers operate in the infrared (IR) and ISM (Industrial, Scientific and Medical) radio bands.

The first standard that was published in 1997 defines three physical layer types [17]. Later, a revised version [2] was released with additional amendments that were published to date. IEEE 802.11a, IEEE 802.11b and IEEE 802.11g are the most common amendments included in this revision. Except for the IEEE 802.11b, which uses DSSS (Direct Sequence Spread Spectrum) modulation, the remaining two are OFDM (Orthogonal Frequency Division Multiplexing) systems. In addition to the revised physical and MAC (Medium Access Control) layer specification, enhancements have been published since then. IEEE 802.11n is the newest OFDM system with MIMO (Multiple-Input-Multiple-Output) capabilities.

The OFDM physical layer is divided into three sublayers [2]. PLCP (physical layer convergence procedure) sublayer is the upper layer providing services to the MAC layer, and PMD (physical medium dependent) is responsible for transmission and reception of PPDU (PLCP protocol data unit) over the physical medium. The third sublayer is PLME (physical layer management entity) which manages the physical layer functions.

Frame structure

The PLCP sublayer communicates with the MAC layer via PSDU (PLCP service data unit), also called MPDU (MAC protocol data unit) from MAC layer side. During transmission, PPDU is formed from PSDU and PLCP preamble. Figure 2.9 shows frame format for OFDM physical layer.

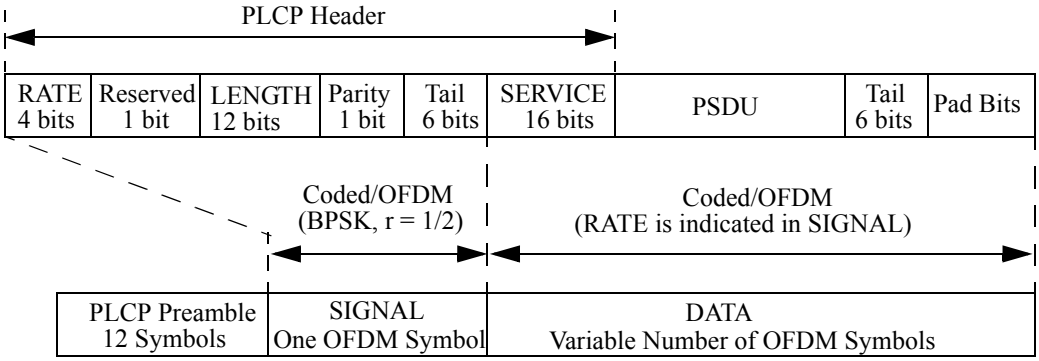

Figure 2.9: PPDU frame structure of OFDM physical layer [2].

PLCP preamble

It comprises 12 OFDM symbols containing training sequences used for synchronization and channel estimation. The first 10 symbols are repetitions of a short sequence for AGC (automatic gain control) convergence, diversity selection, time synchronization and coarse frequency acquisition. After a guard interval, two long sequences are transmitted to aid the receiver estimate the channel and fine frequency offset [2].

PLCP header

The header contains control information appended to PSDU in order to help receiver extract subcarrier modulation type, code rate, payload length and scrambling information.

Data

PSDU from MAC layer is appended to SERVICE field of PLCP header, and then extended with tail bits. The data is then scrambled and encoded with

Rate 1/2 convolutional encoder. Encoded bits are divided into groups each being mapped to complex symbols. Finally, OFDM symbols are formed taking 48 symbols at a time, applying IFFT (Inverse Fast Fourier Transform) and extending them with cyclic prefix. The number of OFDM symbols varies depending on the PSDU length.

2.5 LTE physical layer (Release 8)

LTE uses OFDM modulation at the physical layer. This brings many advantages over modulation techniques used by earlier versions of 3GPP standards such as HSPA/WCDMA and GSM. Since the system bandwidth is divided into independently modulated narrow-band subcarriers, channel fading can be easily mitigated. Over the subcarrier band, the channel response is almost flat so that simple 1-tap channel equalizer can effectively compensate for magnitude and phase distortion. With extended symbol duration (adding cyclic prefix in time domain), multipath fading is avoided. However, OFDM is very sensitive to carrier frequency offset which causes severe inter-carrier interference (ICI). Hence, robust frequency synchronization is required at the receiver.

The physical layer is responsible for mapping of transport layer control information and user data to real physical resources (downlink), and construction of higher level data from electromagnetic signal received via antennas. According to the *physical channels and modulation* specification of LTE [16], the basic components of LTE physical layer on transmission side are channel coding, modulation, precoding, and mapping of symbols onto OFDM subcarriers (resources) of each antenna port. On the other hand, the receiver structure can have different levels of complexity depending on the implementation algorithms. Efficient channel estimation and equalization algorithms are needed in order to achieve good performance in fading environments.

The physical layer specification of LTE [16] defines uplink and downlink physical layer processing functions. Figures 2.10 and 2.11 show the generic block diagrams for uplink (UL) and downlink (DL) transmissions respectively.

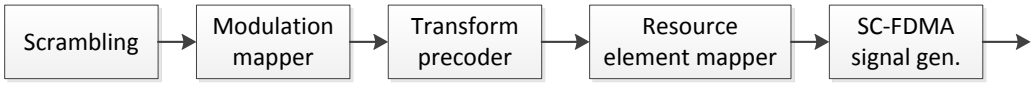

Figure 2.10: Block diagram of uplink physical channel processing.

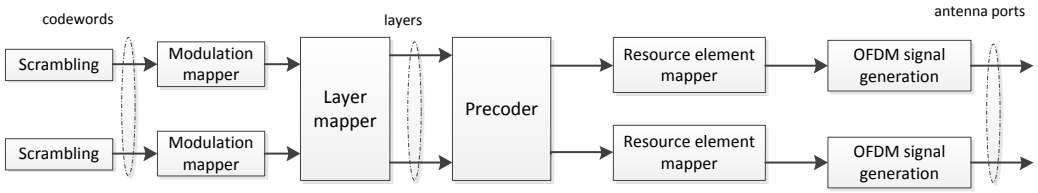

Figure 2.11: Block diagram of downlink physical channel processing.

LTE frame structure

Resources are divided both in time and frequency domain. In time domain, a 10 ms duration is called one frame. In LTE there are two types of frame structures depending whether FDD (Frequency Division Duplexing) or TDD (Time Division Duplexing) is used in UL/DL communication. From now on, we will consider the type-1 (FDD) frame structure shown in Figure 2.12.

A frame is divided into 10 subframes each of which is 1 ms long. There are two 0.5 ms long time slots in every subframe. The 20 time slots in a frame are numbered from 0 to 19.

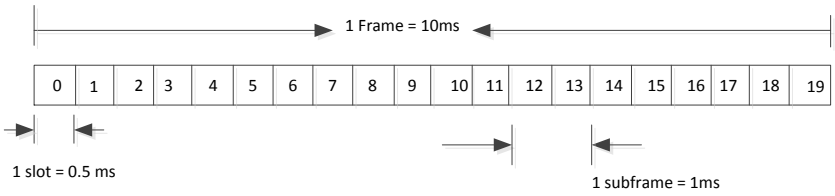

Figure 2.12: LTE frame structure (type-1).

Depending on the cyclic prefix length, there are 6 or 7 OFDM symbols per time slot. Under normal cyclic prefix configuration, there are 7 OFDM symbols per slot. Except for the first symbol, which has 5.2 μs long cyclic prefix, the cyclic prefix is 4.7 μs long for the rest 6 symbols. The useful symbol duration is then 1/15 ms, and hence the subcarrier spacing is 15 kHz. Unless mentioned, a

normal cyclic prefix configuration is assumed.

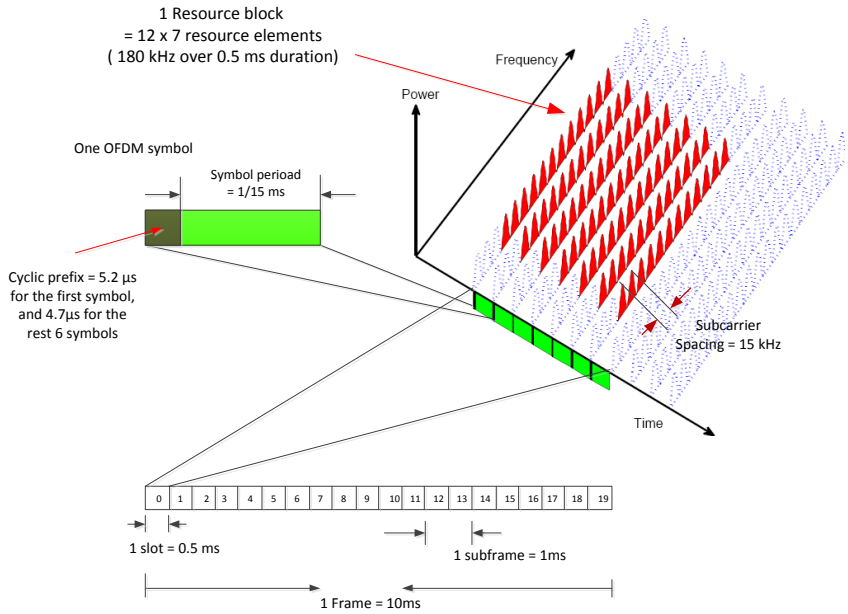

Figure 2.13: Time-frequency resource grid structure of LTE for normal cyclic prefix configuration. In multi-antenna transmission, each antenna port has one resource grid.

Each OFDM symbol carries a set of subcarriers. One subcarrier on a time slot is the smallest time-frequency unit called *resource element*. A group of 12×7 resource elements is called a resource block. This corresponds to 12 subcarriers (or 180 kHz bandwidth) over 7 OFDM symbols as shown in Figure 2.13. The resource elements are mapped to physical channels and physical signals. Reference signals and synchronization signals are the two physical signals used by the physical layer. On the other hand physical channels carry information from the higher layers. The channels carry user data, control information and other signals to the user.

So far we have seen physical layer frame structures of typical OFDM systems which are used in broadcast, wireless local area and cellular networks. Table 2.2 compares OFDM parameters of these systems. Later, Chapter 4 will investigate coexistence issues of these different systems in a shared radio resource.

Parameter	DVB-T	IEEE 802.11-2007	LTE (Release 8)
Channel spacing (MHz)	6, 7, 8	20	1.4, 3, 5, 10, 15, 20
FFT size	2048 (2k mode) 8192 (8k mode)	64	128, 256, 512, 1024, 1536, 2048
Useful subcarriers	1705 (2k mode) 6817 (8k mode)	52	72, 180, 300, 600, 900, 1200
Useful symbol duration, T_U **(**μs**)**	224 (2k mode) 896 (8k mode)	3.2	66.67
Guard interval (μs**)**	$\frac{1}{4}T_U$, $\frac{1}{8}T_U$, $\frac{1}{16}T_U$, $\frac{1}{32}T_U$	$\frac{1}{4}T_U$	5.2 for $l = 0$ 4.7 for $l = 1, 2, \cdots, 6$
Subcarrier spacing (KHz)	4.464 (2k mode) 1.116 (8k mode)	312.5	15
Subcarrier modulation	QPSK, 16QAM, 64QAM, non-uniform 16QAM, non-uniform 64QAM	BPSK, QPSK, 16QAM, 64QAM	QPSK, 16QAM, 64QAM

Table 2.2: Comparison of OFDM parameters of DVB-T, WLAN and LTE physical layers. The parameter l is symbol number in an LTE time slot.

Chapter 3

Cognitive Radios - Interference Channels

In this chapter we will discuss coexistence issues of multiple networks in the shared radio resource. While the frequency band is primarily granted for a licensed user, other secondary users (cognitive radios) access the resource without affecting the primary users. Secondary systems may transmit when other transmitters are not active. Alternatively, the secondary system may transmit simultaneously with the primary transmitter while making sure that the primary system's performance is not degraded. In this type of cognitive radio system, the channel is modeled as interference channel. In the following sections we will briefly discuss forms of secondary spectrum access by cognitive radios. Later, detailed analytical modeling of interference channels and their theoretically achievable capacities are reviewed.

3.1 Secondary spectrum access

The term secondary spectrum access refers to the case where other secondary users try to take advantage of underutilization of the spectrum by the incumbent (primary) users. While it is used by primary users (mostly licensed users), other secondary users (unlicensed users) can access the spectrum without causing intolerable interference to the primary users. Secondary spectrum access mechanisms are devised based on nature of availability of spectrum

and SNR (Signal-to-Noise-Ratio) headroom. In general, the radio frequency spectra can be divided into three groups [7]:

1. *Black spaces* - are occupied bands by high-power users.
2. *Grey spaces* - are partially occupied bands (adjacent bands).
3. *White spaces* - are unoccupied bands by any potential transmitter.

Based on the spectrum occupancy and available information to the cognitive transmitter, a cognitive radio system may *interweave*, *underlay* or *overlay* to the primary transmission.

3.1.1 Interweave system

In this type of cognitive radio, cognitive transmitter first detects whether the spectrum is occupied by other potential transmissions. Detection of these *white spaces* can be, for instance, done by measuring the signal power over a chosen sensing period and comparing it to a threshold value defined. When other sided information about ongoing transmission is known, advanced and more reliable spectrum sensing algorithms can be employed. For example, cyclostationary signals can be detected by autocorrelation of received signals [18], [19]. Moreover, channels occupied by static transmitters such as TV broadcasting stations are known, and geo-location database of these channels is used together with signal detection mechanisms for identifying *white spaces* [20], [21], [22].

Once *white spaces* are identified, cognitive transmitters will be able to use the spectrum for some period of time. This kind of opportunistic spectrum access is accompanied with either continuous spectrum sensing or local database (if applicable) about activity of primary transmitters on that geographical location. The later approach is applied when transmission times of primary users are known beforehand. TV broadcast stations are one of such systems where some channels could be unoccupied for known period of time or in some geographical areas. Figure 3.1 shows possible interweave operation of cognitive radios in *white spaces*. Classification of a given band as *white space* or occu-

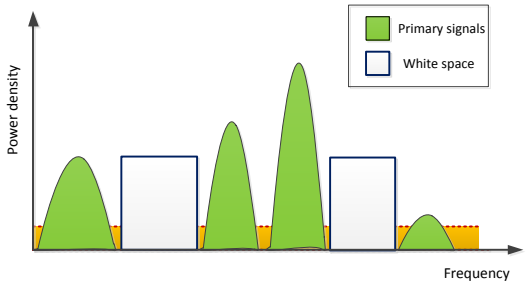

Figure 3.1: Interweave cognitive radio operation - secondary spectrum access on *white spaces*.

pied band is made based on chosen threshold. The decision boundary in this figure is illustrated based on signal power. Other techniques can be used in conjunction to this for more accurate signal detection.

3.1.2 Underlay system

In this type of operation, transmissions from cognitive users can occur while the channels is used by primary transmitters. Transmission power of secondary users is set below the interference threshold for primary receivers [23], [24], [8]. The signal is typically spread over a wide band that could span multiple channels as shown in Figure 3.2. Despreading of secondary signal increases the SNR (Signal-to-Noise-Ratio) at the receiver.

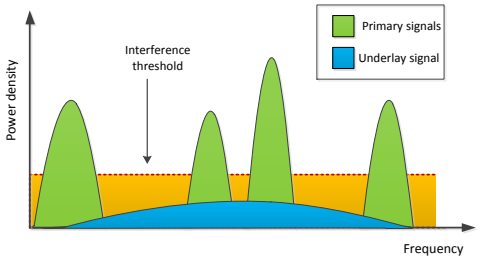

Figure 3.2: Underlay cognitive radio - secondary signal is spread over wide band with low power constrained by interference level tolerated by other non-cognitive users.

3.1.3 Overlay system

This is a more complex type of cognitive radio which operates at the same frequency band simultaneously with the primary system but at low power as shown in Figure 3.3. The overlay system is a special class of interference channel discussed in the following section. Operation of overlay cognitive radio depends on the level of cooperation between the primary and secondary transmitters. It is usually assumed that the secondary transmitter has non-causal message and codebook of the primary transmitter so that it can adapt its transmission accordingly. The secondary transmitter may allocate fraction its power for primary signal to compensate for interference caused by its transmission to the primary receiver. Then, the secondary receiver applies interference cancellation algorithms to remove the primary signal. The capacity gain can be further improved when it is possible to have cooperative coding between the primary and the secondary systems. Detailed analysis of capacity gains of overlay system has been addressed in Chapter 4.

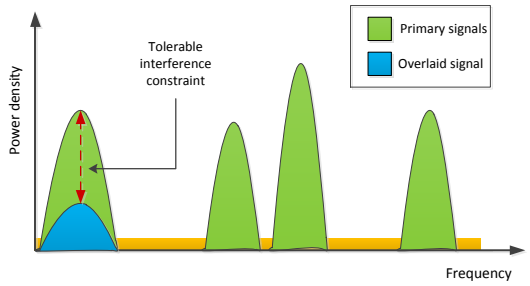

Figure 3.3: Overlay cognitive radio - secondary signal is added on top of the primary signal at relatively low power such that SNR requirement of the primary users is satisfied.

3.2 Interference channel

In overlay cognitive radio systems both the primary and the secondary users transmit simultaneously over a shared radio spectrum thereby interfering each other. The channel of such systems belongs to the class of interference channel with two transmitters and two receivers. This section presents mathematical model of a Gaussian interference channel.

Consider a discrete memoryless two-input-two-output Gaussian interference channel shown in Figure 3.4. The channel has input signals X_1, X_2 and outputs Y_1, Y_2 where the channel has coefficients $h_{ij} \in \mathbb{R}$, $i, j \in \{1,\ 2\}$ with additive Gaussian noises $Z_1 \sim \mathcal{N}(0, N_1)$, $Z_2 \sim \mathcal{N}(0, N_2)$. The transmit symbols X_i are random variables with the following power constraints.

$$E\left\{X_1^2\right\} \leq P_1 \tag{3.1}$$
$$E\left\{X_2^2\right\} \leq P_2 \tag{3.2}$$

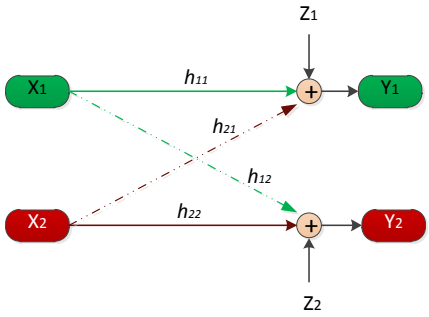

Figure 3.4: Interference channel with two inputs and two outputs.

Outputs of the channel are expressed as

$$Y_1 = h_{11}X_1 + h_{21}X_2 + Z_1 \tag{3.3}$$
$$Y_2 = h_{12}X_1 + h_{22}X_2 + Z_2 \tag{3.4}$$

where the channel coefficients are assumed to be globally known. Let us define the following four variables:

$$SNR_1 = \frac{|h_{11}|^2 P_1}{N_1} \qquad SNR_2 = \frac{|h_{22}|^2 P_2}{N_2} \tag{3.5}$$
$$INR_1 = \frac{|h_{21}|^2 P_2}{N_1} \qquad INR_2 = \frac{|h_{22}|^2 P_1}{N_2} \tag{3.6}$$

where SNR_i is the signal-to-noise ratio at receiver i, and INR_i is interference-to-noise ratio at receiver i, $i \in \{1, 2\}$. The channel can be fully expressed

with power constraints (P_1, P_2), channel coefficients (h_{11}, h_{21}, h_{12}, h_{22}) and noise powers (N_1, N_2). Such a channel can be transformed into equivalent (in terms of capacity) standard form [25] with power constraints (P_1', P_2'), channel coefficients (1, c_{21}, c_{12}, 1) and noise powers (1, 1) where

$$c_{21} = \frac{\sqrt{N_2}}{h_{22}\sqrt{N_1}}h_{21} \qquad c_{12} = \frac{\sqrt{N_1}}{h_{11}\sqrt{N_2}}h_{12} \tag{3.7}$$

$$P_1' = \frac{|h_{11}|^2}{N_1}P_1 \qquad P_2' = \frac{|h_{22}|^2}{N_2}P_2 \tag{3.8}$$

Note that the new power constraints correspond to SNR's at the receivers, i.e. $P_1' = SNR_1$ and $P_2' = SNR_2$.

In interference-free single transmitter-receiver pair communicating over a channel, a rate R is said to be achievable if a message index $\mathcal{M} \in \{1, 2, \cdots, M\}$ can be transmitted using a codeword $\mathbf{x} = (x^{(1)}, x^{(2)}, \cdots x^{(n)})$ with arbitrarily low probability of error in n, sufficiently large, transmissions over the channel where the message alphabet size, M, is an integer greater than or equal to e^{nR}. The maximum achievable rate is called *capacity*, C, of the channel. For AWGN channel, the capacity is given by

$$C = \frac{1}{2}\log\left(1 + \frac{P}{N}\right) \quad \text{nats/s} \tag{3.9}$$

where P is the signal power and N is Gaussian noise power at the receiver.

Similarly for two-input-two-output channel, A rate pair (R_1, R_2) is achievable if two messages $\mathcal{M}_1 \in \{1, 2, \cdots, M_1\}$ and $\mathcal{M}_2 \in \{1, 2, \cdots, M_2\}$ can be transmitted using codewords $\mathbf{x}_1 = (x_1^{(1)}, x_1^{(2)}, \cdots x_1^{(n)})$ and $\mathbf{x}_2 = (x_2^{(1)}, x_2^{(2)}, \cdots x_2^{(n)})$,respectively, with arbitrarily low error probability in sufficiently large n uses of the channel where

$$M_i \geq \lceil e^{nR_i} \rceil \tag{3.10}$$

A set of such achievable rate pairs forms the achievable rate region for the channel under consideration. Achievable rate regions for general interference

channel have been studied in [25]. The region was later extended in [26]. Special case of interference channel were also considered in [27], [13] and [12].

3.3 Orthogonal channel access

The two transmitters shown in Figure 3.4 can share the radio resource orthogonally without interfering each other through FDMA (Frequency Division Multiple Access) and TDMA (Time Division Multiple Access). In these schemes the two senders transmit their messages on different frequency bands or at different instances of time so that the two messages do not interfere with each other. The channel is assumed to be in standard form with power constraints (P_1', P_2'), channel coefficients $(1, c_{12}, c_{21}, 1)$ and additive Gaussian noise powers $(1, 1)$. Let the fraction of the frequency/time resource allocated to sender 1 be β, $0 \leq \beta \leq 1$, and hence sender 2 uses $(1-\beta)$ of the resource. Since the channel is interference free, the achievable rate region is defined by the set of all rate pairs (R_1, R_2) obtained for all values of β, $0 \leq \beta \leq 1$ and satisfying the conditions:

$$R_1 \leq \frac{1}{2}\beta \log\left(1 + \frac{P_1'}{\beta}\right) = C_1 \tag{3.11}$$

$$R_2 \leq \frac{1}{2}(1-\beta) \log\left(1 + \frac{P_2'}{1-\beta}\right) = C_2 \tag{3.12}$$

The capacity region defined by the rate pair is also valid for *interweave* cognitive radios.

3.4 General Gaussian interference channel

In this scenario, two sender-receiver pairs in Gaussian interference channel are considered. Each pairs does not have information about other pair's transmitted codewords. However, joint design of codebooks is allowed. The power constraints and channel coefficients are assumed to be known by both transmitters. Carleial [25] has established the capacity region of such channel through *superposition coding*. The transmitted codeword $\mathbf{x}_i$ of user i is divided into $\mathbf{x}_{i0}$ and $\mathbf{x}_{i1}$ each generated independently from zero mean Gaussian distribution

with variances $(1-\alpha_i)P_i'$ and $\alpha_i P_i'$ respectively. The rate R_i of transmitter i is then the sum of rates R_{i0} and R_{i1} where R_{ij} corresponds to codeword $\mathbf{x}_{ij}$ decoded by receiver i. Received signals after n channel uses are expressed as

$$\mathbf{Y}_1 = \mathbf{X}_{10} + \mathbf{X}_{11} + c_{21}\mathbf{X}_{20} + c_{21}\mathbf{X}_{21} + \mathbf{Z}_1 \tag{3.13}$$

$$\mathbf{Y}_2 = c_{12}\mathbf{X}_{10} + c_{12}\mathbf{X}_{11} + \mathbf{X}_{20} + \mathbf{X}_{21} + \mathbf{Z}_2 \tag{3.14}$$

Carleial [25] suggested four different sequential decoding schemes, (AC), (AD), (BC), & (BD), shown in Figure 3.5 where $\mathbf{Y}_1$ can be decoded by either (A) or (C). Similarly, (C) and (D) are two possible decoders for $\mathbf{Y}_2$. From these schemes, four achievable rate pairs can be found for some $(\alpha_1, \alpha_2) \in [0,1]^2$. Each receiver has a set of maximum likelihood decoders. The rate constraint

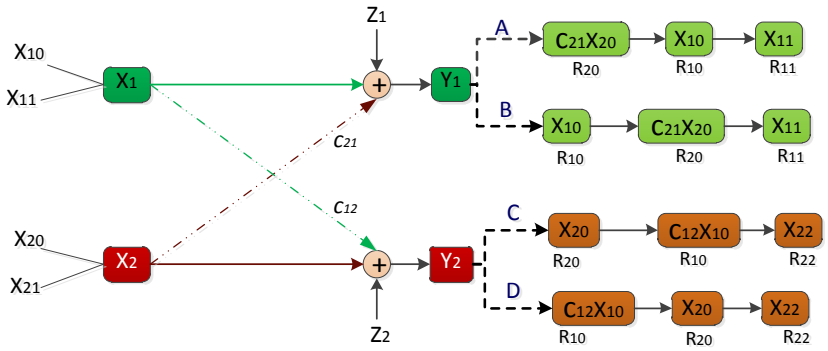

Figure 3.5: Sequential decoding schemes of Gaussian interference channel.

on a decoder make sure that it decodes the codeword with arbitrarily small probability of error and input signal to succeeding decoders does not contain interference from previously decoded codewords. Therefore, we will have three constraints on each receiver. For example, the rate constraints scheme (AC)

are given by

$$R_{10} \leq \frac{1}{2}\log\left[1+(1-\alpha_1)P_1'/(1+\alpha_1 P_1'+a_{21}P_2')\right] \tag{3.15}$$

$$R_{20} \leq \frac{1}{2}\log\left[1+a_{21}(1-\alpha_2)P_2'/(1+\alpha_1 P_1'+a_{21}\alpha_2 P_2')\right] \tag{3.16}$$

$$R_{11} \leq \frac{1}{2}\log\left[1+\alpha_1 P_1'/(1+a_{21}\alpha_2 P_2')\right] \tag{3.17}$$

$$R_{20} \leq \frac{1}{2}\log\left[1+(1-\alpha_2)P_2'/(1+a_{12}P_1'+\alpha_2 P_2')\right] \tag{3.18}$$

$$R_{10} \leq \frac{1}{2}\log\left[1+a_{12}(1-\alpha_1)P_1'/(1+a_{12}\alpha_1 P_1'+\alpha_2 P_2')\right] \tag{3.19}$$

$$R_{22} \leq \frac{1}{2}\log\left[1+\alpha_2 P_2'/(1+a_{12}\alpha_1 P_1')\right] \tag{3.20}$$

where $a_{ij} = |c_{ij}|^2$. Constraints on achievable rate pairs ($R_1 = R_{10} + R_{11}$, $R_2 = R_{20} + R_{21}$) are expressed by combining the above constraints as

$$\begin{aligned} R_1 \leq \frac{1}{2}\,\mathsf{min}\,\{&\log\left[1+(1-\alpha_1)P_1'/(1+\alpha_1 P_1'+a_{21}P_2')\right], \\ &\log\left[1+a_{12}(1-\alpha_1)P_1'/(1+a_{12}\alpha_1 P_1'+\alpha_2 P_2')\right]\} + \\ &\log\left[1+\alpha_1 P_1'/(1+a_{21}\alpha_2 P_2')\right] \end{aligned} \tag{3.21}$$

$$\begin{aligned} R_2 \leq \frac{1}{2}\,\mathsf{min}\,\{&\log\left[1+a_{21}(1-\alpha_2)P_2'/(1+\alpha_1 P_1'+a_{21}\alpha_2 P_2')\right], \\ &\log\left[1+(1-\alpha_2)P_2'/(1+a_{12}P_1'+\alpha_2 P_2')\right]\} + \\ &\log\left[1+\alpha_2 P_2'/(1+a_{12}\alpha_1 P_1')\right] \end{aligned} \tag{3.22}$$

Four such achievable rate pairs are obtained from receiver schemes, (AC), (AD), (BC) & (BD) . The achievable rate region is bounded by the set of achievable rate pairs for every $(\alpha_1, \alpha_2) \in [0,1]^2$. Carleial [25] also showed that in strong interference scenarios where $a_{12} \geq 1 + P_2'$ and $a_{21} \geq 1 + P_1'$, the achievable rate region coincides with capacity region of interference-free channel:

$$R_1 \leq \frac{1}{2}\log(1+P_1') \qquad R_2 \leq \frac{1}{2}\log(1+P_2') \tag{3.23}$$

Carleial's rate region was based on *sequential* superposition coding [26]. Han and Kobayashi [26] have obtained relaxed rate region using *simultaneous* superposition coding. The reader is referred to [26] for detailed explanation.

Consequently, they have also established generalized form for the rate region given in Equation (3.23) for all $a_{12}, a_{21} \geq 1$ bounded by the following constraints

$$R_1 \leq \frac{1}{2}\log(1+P_1') \tag{3.24}$$

$$R_2 \leq \frac{1}{2}\log(1+P_2') \tag{3.25}$$

$$R_1+R_2 \leq \frac{1}{2}\min\left\{\log(1+P_1'+a_{12}P_2'), \log(1+P_2'+a_{12}P_1')\right\} \tag{3.26}$$

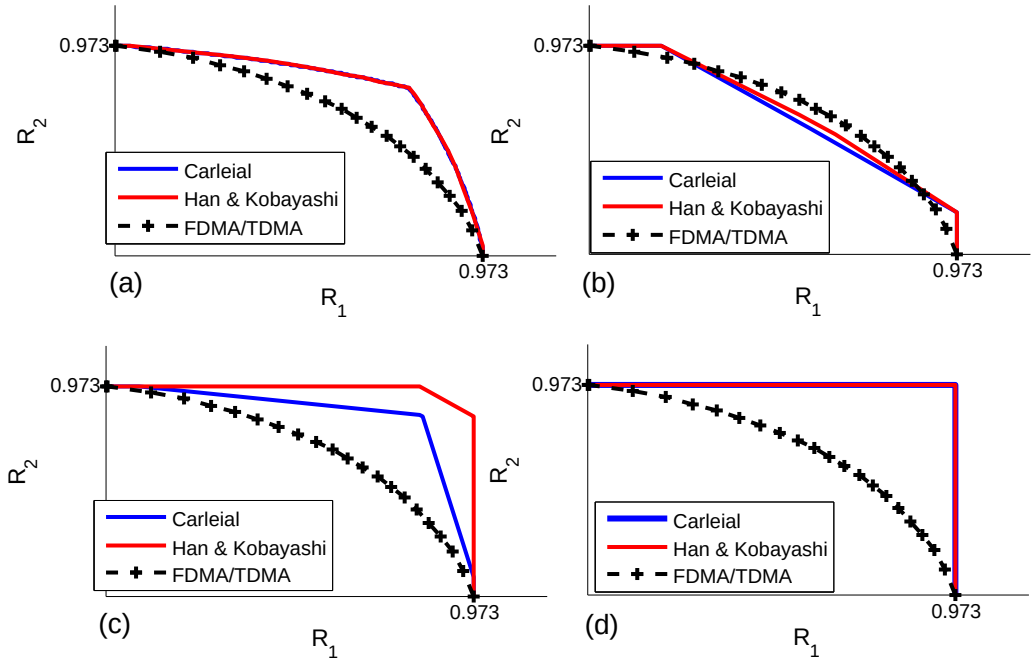

Figure 3.6: Bounds for achievable rate regions for general Gaussian interference channel: (a) $P_1' = P_2' = 6,\ a_{12} = a_{21} = 0.1$, (b) $P_1' = P_2' = 6,\ a_{12} = a_{21} = 0.55$, (c) $P_1' = P_2' = 6,\ a_{12} = a_{21} = 5$ (d) $P_1' = P_2' = 6,\ a_{12} = a_{21} = 7$.

Figure 3.6 shows boundaries of achievable rate regions for different interference levels. Han and Kobayashi's achievable rate region (red line) subsumes Carleial's (blue line). As can be seen from Figure 3.6, capacity region of interference channels converges to that of interference-free channel ($a_{12} = a_{21} = 0$) in very weak, (a), and very strong, (c) and (d), interference scenarios. The latter is due to the fact that, a receiver can effectively decode the interference

and subtract it from the received signal before decoding its own message. However, orthogonal channel access via FDMA or TDMA (shown with black dots) can achieve higher rate than *simultaneous* superposition coding in moderate interference power.

Chapter 4

Overlay Cognitive Radio

As seen in the previous chapter, orthogonal channel access is not necessarily optimal in achieving channel capacity. Results from [25], [26] and [28] have shown that non-orthogonal transmissions are optimal in most situations. For example, in strong interference scenario, the receiver can effectively cancel the interference through successive decoding. The interfering user's data is first decoded and estimate of the signal from this user is subtracted from the received signal. Then, the other user's data is decoded from the residual signal.

Overlay transmission is a non-orthogonal channel access techniques used in cognitive radios. In overlay cognitive radio, both the primary and the cognitive users transmit over the same frequency band simultaneously. The cognitive transmitter operates within the coverage area of the primary transmitter, as illustrated in Figure 4.1, under the constraint that it will not affect the primary users. The cognitive transmitter is required to relay the primary signal (in addition to transmitting its own signal) to maintain the SNR requirement of the primary receiver. It is usually assumed that the primary receiver is unaware of existence of the cognitive transmitter. The primary receiver, therefore, does not cooperate with the secondary system. Moreover, the primary transmitter's cooperation is very limited. The primary transmitter might, for example, provide the secondary transmitter with primary message before its transmission such that the secondary transmitter can adapt its transmission accordingly.

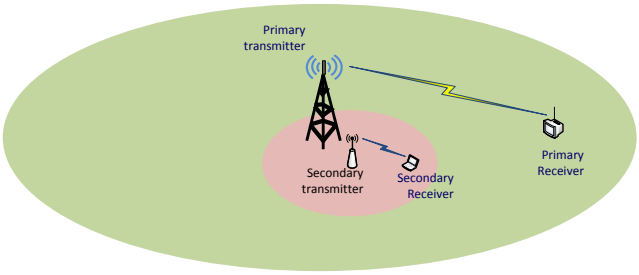

Figure 4.1: Concurrent operation of secondary system (cognitive) within the coverage area of primary system.

In this chapter, we will build up theoretical analysis of cognitive radio channels. Mathematical models and achievable capacities for such channels are studied. Later, some of limitations during practical implementation are discussed. Finally, the proposed overlay transmitter and receiver chosen based on constraints by the implementation of the system is presented. Throughout this chapter, the names, *cognitive* and *secondary*, are used interchangeably in the context of secondary spectrum access via cognitive radio.

4.1 Overlay cognitive radio Gaussian channel

This is special class of Gaussian interference channel. In the simplest configuration having only one secondary user, it is a two-input-two-output interference channel with asymmetric side information at the second transmitter as depicted in Figure 4.2. Sender 2 (cognitive transmitter) has knowledge of primary transmitter's message and can adapt its transmission accordingly. The primary receiver is unaware of existence of the cognitive transmitter. On the other hand, the cognitive (secondary) transmitter-receiver pair operate against interference caused by the primary transmission to maximize transmission rate while ensuring the primary receiver is not affected.

Consider a standard form cognitive Gaussian channel shown in Figure 4.2 with power constraints (P'_p, P'_s), channel coefficients $(1, c_{21}, c_{12}, 1)$ and noise powers $(1, 1)$. Capacity of primary system in the absence of interference, $c_{21} = 0$, is

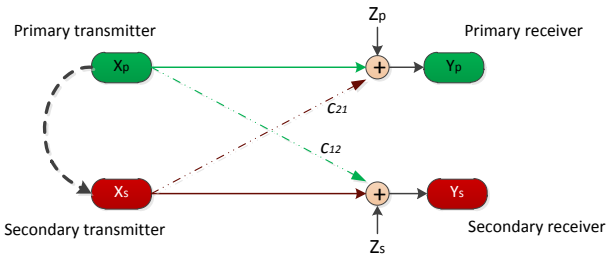

Figure 4.2: A two-input-two-output Gaussian interference channel with the second transmitter having non-causal messages of the primary.

given by

$$C_1 = \frac{1}{2}\log(1+P_p') \tag{4.1}$$

Overlay cognitive radio operates under the constraint that primary system's capacity, C_1, remains unaffected. The cognitive transmitter overlays its message on top of the primary signal at carefully chosen power level that the primary receiver can tolerate. For instance, the cognitive transmitter might relay the primary transmission by allocating part of its power for the primary signal. Let α be the fraction of cognitive transmitter's power allocated to the relayed primary signal. The transmitted signal at the cognitive transmitter is expressed as

$$X_s = X_c + \sqrt{\frac{\alpha P_s'}{P_p'}} X_p \tag{4.2}$$

where X_p is the primary signal relayed by the cognitive transmitter, X_c is cognitive transmitter's own signal. X_p and X_s are assumed to be independently

distributed random variables. Outputs of the channel are given by

$$\begin{aligned} Y_p &= X_p + c_{21}\left(X_c + \sqrt{\alpha P_s'/P_p'}X_p\right) + Z_p \\ &= \left[1 + c_{21}\sqrt{\alpha P_s'/P_p'}\right] X_p + c_{21}X_c + Z_p \qquad (4.3) \\ Y_s &= X_c + \sqrt{\alpha P_s'/P_p'}X_p + c_{12}X_p + Z_s \\ &= X_c + \left[c_{12} + \sqrt{\alpha P_s'/P_p'}\right] X_p + Z_s \qquad (4.4) \end{aligned}$$

When channel coefficients are positive and real, the primary signals received from the primary transmitter and the one relayed by the secondary transmitter are added coherently at the receiver. This also holds when the secondary transmitter has perfect knowledge of the channel coefficients. Therefore, the received primary signal power at the primary receiver becomes $(\sqrt{P_p'}+|c_{21}|\sqrt{\alpha P_s'})^2$, and interference power at the primary receiver is $|c_{21}|^2(1-\alpha)P_s'$. Assuming cognitive transmitter's signal, X_c, appears Gaussian to the primary receiver, capacity of the primary system takes the form

$$R_1(\alpha) = \frac{1}{2}\log\left(1 + \frac{(\sqrt{P_p'} + |c_{21}|\sqrt{\alpha P_s'})^2}{1 + |c_{21}|^2(1-\alpha)P_s'}\right) \qquad (4.5)$$

where the value of α is chosen to meet the capacity requirement of primary system given in Equation (4.1). Hence

$$\alpha^* = \left(\frac{\sqrt{P_p'}\left(\sqrt{1 + |c_{21}|^2 P_s(1+P_p')} - 1\right)}{|c_{21}|\sqrt{P_s'}(1+P_p')}\right)^2 \qquad (4.6)$$

4.2 Achievable capacity

Due to availability of side-information at the cognitive transmitter, the achievable rate region subsumes that of general interference channel obtained in [26]. Achievable capacity of cognitive radio channel has been studied in [28]. Costa [28] has shown that *dirty-paper* coding can achieve a rate equivalent

to interference-free capacity. In this setting, the primary signal is treated as non-causally known Gaussian interference, S, to the cognitive transmitter as depicted in Figure 4.3. The received signal by the cognitive user is expressed as

$$Y = X + S + Z \tag{4.7}$$

where X is transmitted signal by the cognitive transmitter, and Z is additive Gaussian noise.

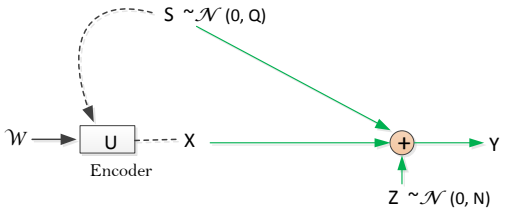

Figure 4.3: Dirty-paper coding with additive Gaussian noise and Gaussian distributed interference, S, known by the transmitter. Power of the transmitted signal, $X = U - \alpha S$, is constrained by $(1/n)\sum_{i=1}^{n} X_i^2 \leq P$.

For each message $\mathcal{W} \in \{1, 2, \cdots, W\}$ to be transmitted in n sample times, the encoder chooses an auxiliary codeword $\mathbf{u} \in \mathbf{U}$ such that the transmitted codeword $\mathbf{x} = \mathbf{u} - \alpha\mathbf{s}$ is nearly orthogonal to the interference $\mathbf{s}$. The codebook $\mathbf{U}$ is known by both the transmitter and the receiver. The rate is maximized when $\alpha = P/(P + N)$. As $n \to \infty$, the rate converges to

$$R_{max} = \frac{1}{2}\log(1 + P/N) \tag{4.8}$$

Devroye et al. [13] obtained achievable rate region for cognitive radio channels via superposition coding scheme used in [26] except that the second transmitter performs *dirty-paper* coding [28] on each sub-codeword. Transmitted codeword by the primary transmitter $\mathbf{x}_1$ is divided into $\mathbf{x}_{10}$ and $\mathbf{x}_{11}$ each generated independently from zero mean Gaussian distribution with variances $(1 - \mu_1)P_1$ and $\mu_1 P_1$ respectively. On the other hand, codewords of the cognitive transmitter, $\mathbf{x}_{20} \sim \mathcal{N}(0, (1 - \mu_2)P_2)$ and $\mathbf{x}_{21} \sim \mathcal{N}(0, \mu_2 P_2)$ are formed

using Costa's *dirty-paper* coding [28].

$$\mathbf{x}_{20} = \mathbf{u}_1 - \alpha_0 \mathbf{x}_1 \tag{4.9}$$

$$\mathbf{x}_{21} = \mathbf{u}_2 - \alpha_1 \mathbf{x}_1 \tag{4.10}$$

The achievable rate region is defined by set of constraints on rates, $\{R_{11}, R_{12}, R_{21}, R_{22}\}$, derived by following similar procedure used in [26]. The reader is referred to [13] for derivation of rate constraints.

It is often assumed that the primary system's operation should be independent of other cognitive users. In general, the following constraints are considered in an overlay cognitive radio channel.

- The primary receiver uses single user decoder and is assumed to be unaware of existence of the cognitive transmitter.
- The secondary transmitter has to allocate fraction, α^*, of its power to relay the primary signal such that the primary receiver sees the same SNR in the presence of the secondary transmitter as in its absence.
- The cognitive transmitter can only acquire messages of the primary transmitter and no joint codebook design is allowed.

Under these constraints, the rate for the primary transmitter is given by

$$R_1(\alpha^*) = \frac{1}{2}\log(1 + P_p') \tag{4.11}$$

On the other hand, rate of the cognitive transmitter is maximized through *dirty-paper* coding provided that the cognitive transmitter has knowledge of the channel coefficients.

$$R_2(\alpha^*) = \frac{1}{2}\log\left(1 + (1 - \alpha^*)P_s'\right) \tag{4.12}$$

It has been shown in [12] that the rate $R_2(\alpha^*)$ is capacity of a cognitive radio channel without the second constraint when the interference is low, $c_{21} \leq 1$. In additive Gaussian noise, interference-free capacity has been found to be

achievable for general non-causally known interference [29].

Costa's result [28] was based on the assumption that the transmitter knows the whole interference sequence at beginning of transmission. Another setting is the case where the transmitter cannot access future signals to be transmitted by the primary transmitter. On i^{th} use of the channel, the transmitter knows interference signals, $s_1, s_2, \cdots, s_i$ only. Capacity of causally known *dirty-tap* channel [30] was studied by Shannon [31]. For any noise Z, $E\{Z^2\} = N$ and causally known general interference, closed form expression for lower-bound of the capacity has been derived in [30] to be

$$C_{causal} \geq \frac{1}{2}\log(1 + P/N) - \frac{1}{2}\log\frac{2\pi e}{12} \tag{4.13}$$

$$C_{causal} \geq \frac{1}{2}\log(1 + P/N) - 0.1765 \tag{4.14}$$

For causally known Gaussian interference S, $E\{S^2\} = Q$, Willems [32] was the first to propose a coding scheme based on scalar quantization. In his coding scheme, the transmitter uses fraction of its power to 'concentrate' the interference to one of points in equally spaced lattice $\{\cdots, -2A, -A, 0, A, 2A, \cdots\}$ such that the decoder can identify the interference when $A^2 >> N$ where N is the Gaussian noise power. By incorporating a random dither at the encoder, the received signal could be made independent of the interference distribution [30]. The drawback of this scheme is that the transmitter loses fraction of its power, $\approx A^2/12$ when $A^2 << Q$, to quantize the interference. Realization of *dirty-paper* coding through *multidimensional lattice quantization* has been given in [29].

4.3 Practical considerations

Unlike MIMO broadcast systems, primary and secondary transmitters of cognitive radio cannot jointly design their codes. Therefore, the secondary system alone should be designed to effectively communicate under the primary system's interference. When the secondary transmitter can acquire the primary message, interference avoidance or mitigation techniques can be applied based

on this side information during transmission. This helps the secondary receiver easily decode the message. On the other hand, when such prior information is unavailable, the secondary system's performance relies on the receiver. If the interference is very strong, the receiver may, for example, estimate the interference and subtract it from the received signal.

Dirty-paper coding proposed for transmitter side precoding assumes that the channel coefficients are known by the transmitter. This is in practice difficult due to the fact that the secondary receiver has to estimate channel gains from the primary and the secondary transmitters separately and send the feedback. Moreover, practical implementation of near-capacity coding schemes require joint design of source and channel codes. In this thesis, we focus on practical implementation of the physical layer. Complex channel coding schemes are beyond the scope of this thesis. Moreover, the SNR constraint on the primary signal ensures that the the primary signal is strong enough to be decoded by the secondary receiver with low probability of error. Therefore, in such high-interference situation, a simple sequential decoding by the secondary receiver achieves acceptable performance which is close to interference-free scenario. In the following sections, we present transmitter and receiver implementation based on sequential decoding strategy.

Primary system characteristics

We consider the DVB transmitter as a primary user. Each of the transmitted OFDM symbols carry one MPEG-2 transport stream packets. Two types of reference pilots for channel estimation are transmitted over a set of OFDM carriers. Location of first set of pilot signals, called *continual pilots*, is fixed while *scattered pilots* change their location from symbol to symbol as shown in Figure 4.4. The receiver uses both pilots to estimate the channel. When there is overlay transmission on these carriers, the receiver's equalizer suffers from interference caused by secondary transmission. Moreover, the secondary receiver cannot easily extract the secondary signal due to channel estimation errors. To study the effect of secondary transmission on pilot carriers, we will consider two types of overlay cognitive radios.

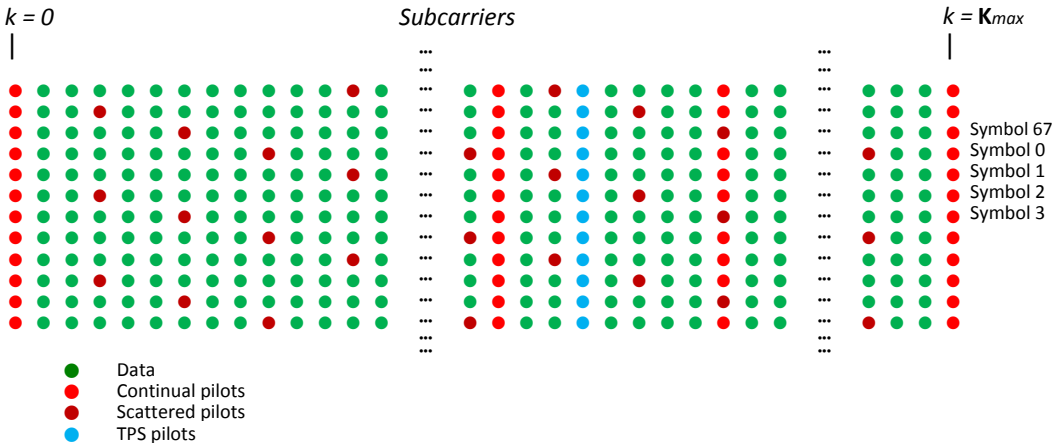

Figure 4.4: Illustration of DVB signal pilot structure. Unlike *scattered pilots*, *continual pilots* have fixed locations.

Orthogonal pilots

In this scenario, the secondary transmission is orthogonal to the primary pilot carriers. For ease of implementation, the secondary system skips only *continual pilots* since *scattered pilots* change their locations dynamically, and this causes additional complexity on the secondary receiver. We take an OFDM based WLAN-type secondary transmitter as a candidate for *orthogonal pilot* overlay scheme shown in Figure 4.5. In this transmitter, a MAC layer packet is transmitted over a number of successive OFDM symbols. Transmissions are initiated at any time in discontinuous fashion. A known pilot sequence, *preamble*, is transmitted at the beginning each transmission. The preamble is used for synchronization and channel estimation. The secondary transmission is made in such a way that in all OFDM symbols including the preamble, no transmission occurs on of the primary transmitter's *continual pilot* carriers.

Non-orthogonal pilots

In non-orthogonal overlay transmission, the secondary transmitter uses all carriers. On one hand, this approach allows for usage of more resources unlike orthogonal transmissions. On the other hand, however, it becomes difficult for the secondary receiver to estimate channels of the primary and the secondary signals separately. Therefore, the secondary receiver's performance might be

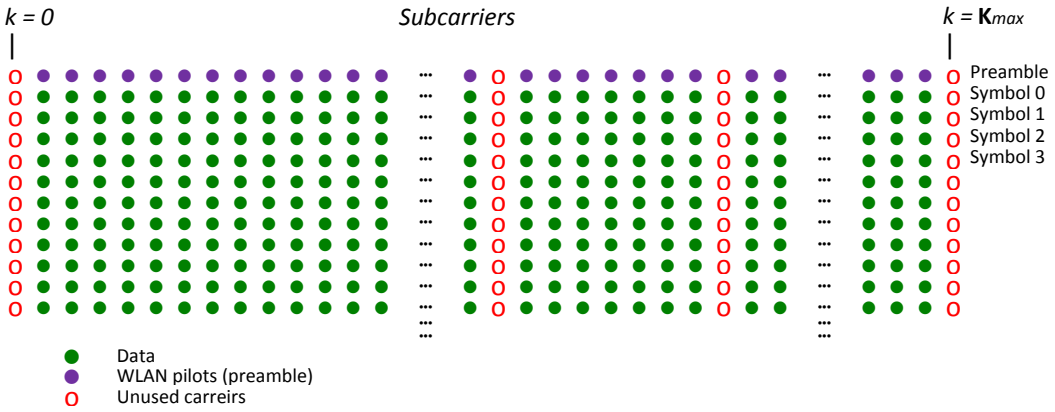

Figure 4.5: Proposed WLAN-type frame structure for *orthogonal pilot* overlay cognitive radio.

severely degraded.

An LTE-type transmitter is proposed for *non-orthogonal pilot* type of overlay transmission. Figure 4.6 shows LTE-type frame structure. LTE physical layer frame is divided into subframes each of which contains 14 OFDM symbols. Pilot signals which are used for channel estimation are transmitted on defined set of carriers. According to the LTE physical layer specification [16], these pilots are distributed in time and frequency, and hence their location varies from one OFDM symbol to another. Therefore, they overlap with primary pilot signals. Since the secondary receiver relies on these pilots, they cannot be suppressed to enable *orthogonal pilot* transmission. Due to this fact, it is reasonable to consider *non-orthogonal pilot* scheme for such secondary system.

4.4 Overlay transmitter

The proposed cognitive transmitter superimposes the primary and the secondary signals as depicted in Figure 4.7. The overlay operation adds the two symbols, X_p and X_c, which are scaled by factors chosen to divide the transmitter's power. The transmitter allocates fraction of its power, $\alpha^* P_s$, for the primary message, and the rest $(1 - \alpha^*)P_s$ for its own message, and hence the

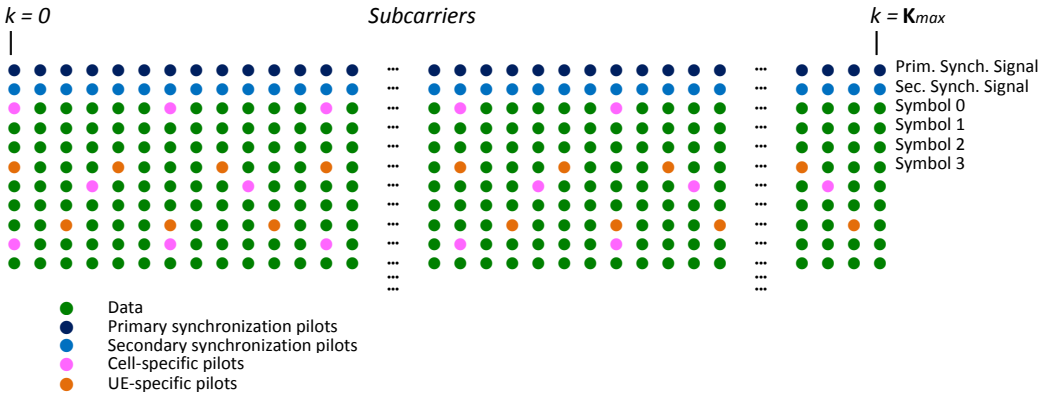

Figure 4.6: LTE-type frame structure with synchronization symbols and reference pilots.

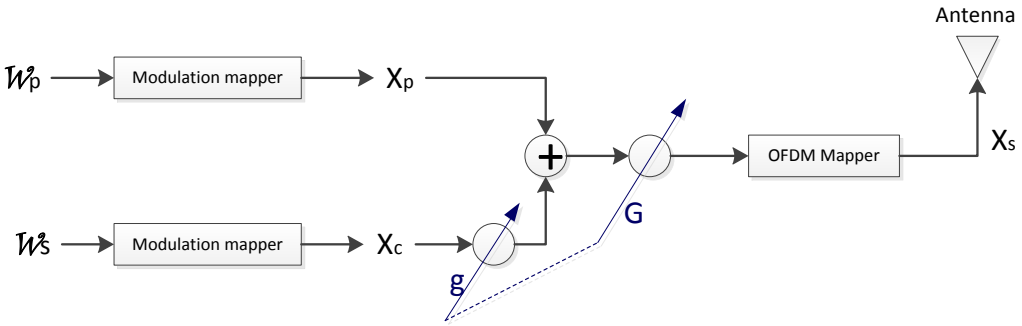

Figure 4.7: Overlay transmitter design where $\mathcal{W}_p$ is the primary message encoded to X_p, and $\mathcal{W}_s$ is the secondary message encoded to X_c. The scaling factors, g and G, are calculated based on the power constraints, P_p and P_s, and relaying fraction, α^*, obtained in Equation (4.6).

transmitted signal is expressed as

$$X_s = X_c + \sqrt{\frac{\alpha^* P_s}{P_p}} X_p \tag{4.15}$$

The relaying fraction, α^*, given in Equation (4.6) is for a standard-form channel. To simplify expressions, we will consider non-standard form channel in remaining parts of this text. Let the channel have power constraints (P_p, P_s), channel coefficients (h_{11}, h_{21}, h_{12}, h_{22}) and noise powers (N_p, N_s). The

corresponding relaying fraction, λ^*, is expressed as

$$\lambda^* = \left(\frac{|h_{11}|\sqrt{P_p}\left[\sqrt{N_p^2 + P_s\left(N_p + |h_{11}|^2 P_p\right)} - N_p\right]}{|h_{21}|^2\sqrt{P_s}\left(N_p + |h_{11}|^2 P_p\right)} \right)^2 \tag{4.16}$$

The optimal scaling factor, g, in Figure 4.7 can be derived from Equation (4.15), and it is given by

$$g = \sqrt{P_p/\lambda^* P_s} \tag{4.17}$$

4.5 Overlay receiver

The overlay receiver relies on the condition that the primary signal is strong enough (compared to secondary signal and noise powers) such that it can be decoded with very low probability of error. The receiver decodes the secondary message in a two-step process as shown in Figure 4.8. First the primary signal, $\hat{X}_p$, is estimated and subtracted from the equalized signal, Y_c. Then another detector is used to estimate the secondary signal.

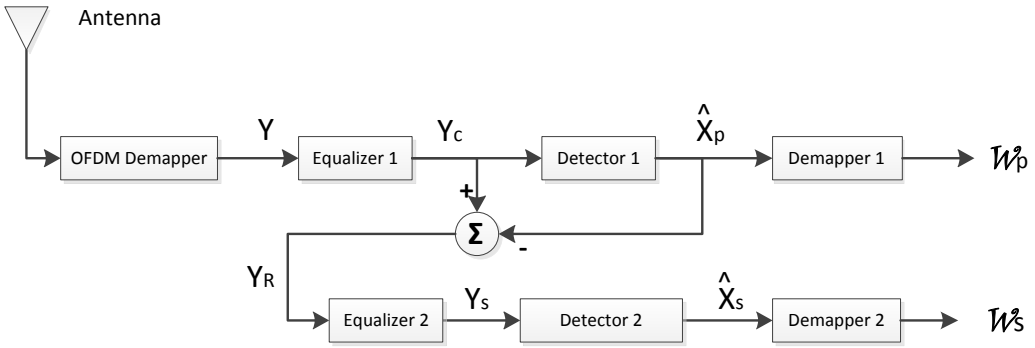

Figure 4.8: Sequential decoding of secondary message. The equalizer estimates the channel using pilots of the primary signal.

The received signal, Y, is written as

$$Y = \left[h_{12} + h_{22}\sqrt{\lambda^* P_s/P_p}\right] X_p + h_{22}X_c + Z_s \tag{4.18}$$

$$= H_p X_p + h_{22}X_c + Z_s \tag{4.19}$$

where the channel coefficient of the primary signal, H_p, is given by

$$H_p = h_{12} + h_{22}\sqrt{\lambda^* P_s/P_p} \tag{4.20}$$

In order to detect transmitted signal, the receiver has to know amplitude and phase distortion caused by the channel. In OFDM signal, the channel frequency response on each subcarrier is represented by complex number. In many OFDM based systems, globally known pilot signals are transmitted on a set of subcarriers in order to aid channel estimation. The channel coefficients on adjacent data subcarriers are computed by interpolating estimates from pilots. Accuracy of channel estimates improves when more pilots are inserted; however, this leads to loss of capacity due to extra signalling overhead.

Channel equalization compensates for distortion due to the channel by multiplying the received signal with equalization coefficient, β. The equalized signal takes the form

$$Y_c = \beta Y \tag{4.21}$$

$$= \beta H_p X_p + \beta h_{22}X_c + \beta Z_s \tag{4.22}$$

A well known equalizer is the minimum mean-square error (MMSE) algorithm. MMSE equalizing coefficient is chosen such that the mean-square error (MSE) given in Equation (4.23) is minimized.

$$E\left\{\left|\beta Y - X_p\right|^2\right\} \tag{4.23}$$

Assuming that data symbols, X_p, are statistically independent with zero-mean

and power, P_p, the MMSE coefficient becomes [3]

$$\beta_{MMSE} = \frac{H_p^*}{|H_p|^2 + N_s/P_p} \tag{4.24}$$

One of the drawbacks of MMSE equalizer is that it requires knowledge of SNR at the receiver. Moreover, the channel distortion is not removed completely. An alternative approach is the Zero-Forcing (ZF) equalizer which tries to completely compensate for the channel. The ZF equalizing coefficient, β_{ZF}, is inverse of the channel coefficient:

$$\beta_{ZF} = \frac{1}{H_p} \tag{4.25}$$

In pilot-based channel estimation, the channel coefficients on pilot carriers are first computed. The simplest approach to calculate these channel coefficients is to divide the received signal by the known pilot symbol value.

In *orthogonal pilot* overlay scheme, the secondary user does not transmit its own data on subcarriers allocated for primary transmitter's pilots, rather it simply relays the primary signal with fraction of its power. The received signal on these pilot locations contains only the primary signal and additive Gaussian noise. It is expressed as

$$Y^p = \left[h_{12} + h_{22}\sqrt{\lambda^* P_s/P_p}\right] X_p + Z_s \tag{4.26}$$

$$= H_p X_p + Z_s \tag{4.27}$$

Estimate of the channel coefficient becomes

$$\tilde{H}_p = \frac{Y^p}{X_p} \tag{4.28}$$

$$= H_p + \frac{Z_s}{X_p} \tag{4.29}$$

When the SNR is strong, effect of the latter term in Equation (4.28) can be neglected. Therefore, sufficiently close channel estimate can be easily obtained.

On the other hand, in *non-orthogonal pilot* overlay scheme, the situation is different. In this case, the received signal also contains the secondary transmitter's own signal. The received signal on primary pilot carriers is similar to the one given in Equation 4.18. The instantaneous channel estimate on a given pilot carrier would look like

$$\tilde{H}_p = \frac{Y}{X_p} \tag{4.30}$$

$$= H_p + \frac{h_{22}X_c}{X_p} + \frac{Z_s}{X_p} \tag{4.31}$$

Even though the secondary signal, X_c, is weaker than the primary signal, X_p, its effect on the channel estimate cannot be ignored. Moreover, equalizing the channel with this estimate discriminates the secondary signal, X_c, on the residual output of the equalizer which is needed to decode the secondary signal. To overcome this problem, the channel estimates, $\tilde{H}_p$, are filtered using a 1-tap low-pass filter.

Let $\tilde{H}_p^i$ be the channel estimate on a given subcarrier of the i^{th} OFDM symbol. The corresponding filtered channel estimate during i^{th} OFDM symbol is

$$\hat{H}_p^i = \rho\hat{H}_p^{i-1} + (1-\rho)\tilde{H}_p^i, \quad 0 \leq \rho \leq 1 \tag{4.32}$$

There is a trade-off between channel tracking capability and elimination of effect of the secondary signal, X_c, on the channel estimate. When the channel forgetting factor, ρ, is increased, the channel coefficient estimate becomes less sensitive to the secondary signal, X_c, though it leads to poor channel estimate in fast fading environment.

Since pilots are scattered in time and frequency domains, channel responses on other subcarriers should be estimated based on channel estimates of adjacent pilots. One way to do this is by applying two-dimensional interpolation. The popular technique is Wiener filter whose coefficients are computed based on MMSE criterion.

The drawback of two-dimensional filtering is complexity due to computations involving large matrices. An alternative approach is cascaded one-dimensional interpolation. Channel estimates for subcarriers of an OFDM symbol are first obtained from frequency-domain interpolation. Then time-domain interpolation is applied for successive OFDM symbols. The order of time and frequency domain interpolations can be interchanged. These interpolators can be implemented using one-dimensional Wiener filter which is optimal in MMSE sense. However, the filter coefficients are dependent on channel statistics and noise variance [3]. Moreover, the time-domain filter introduces additional delay since all OFDM symbols in a block should be received in order to extract pilots required for computation of filter coefficients. In frequency-domain, a Least Squares (LS) based interpolation can be used to fully exploit channel estimates of all pilots in the OFDM symbol. On the other hand, time-domain piecewise polynomial interpolation based on few taps minimizes filtering delay while providing acceptable performance. Figure 4.9 illustrates possible time-domain filter implementations.

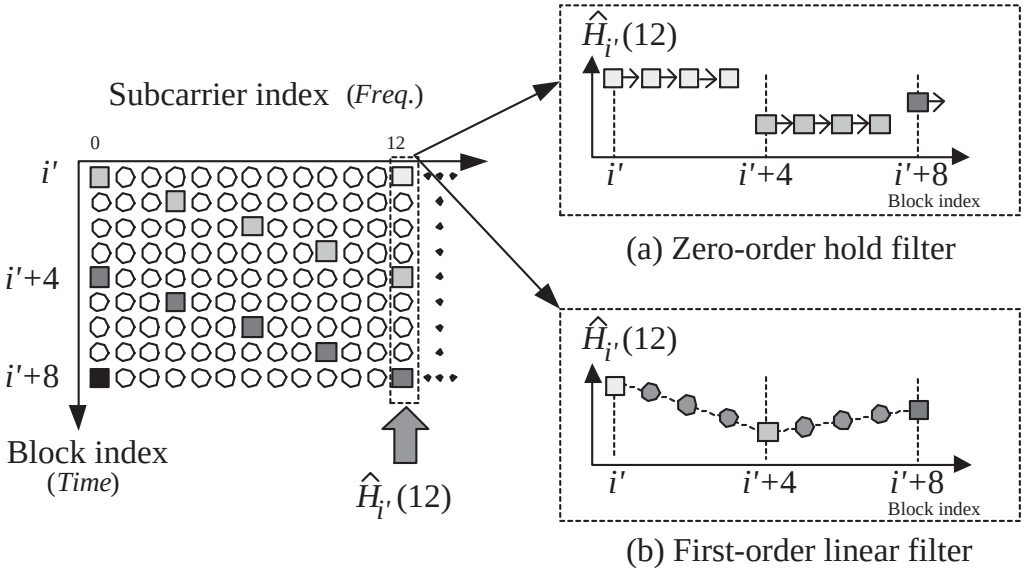

Figure 4.9: Time-domain interpolation using (a) zero-order and (b) first-order polynomial filters [3].

Output of the first equalizer in Figure 4.8, (*Equalizer 1*), can be expressed as

$$Y_c = (1 - \epsilon_p)X_p + \beta h_{22} X_c + \beta Z_s \tag{4.33}$$

where ϵ_p accounts for channel estimation error for the primary signal.

$$\epsilon_p = 1 - \frac{H_p}{\hat{H}_p} \tag{4.34}$$

Input to the second equalizer is the residual signal, Y_R, which is obtained after the quantized primary signal, $\hat{X}_p$, is subtracted from the equalizer output.

$$Y_R = \beta h_{22} X_c + \delta + \beta Z_s, \qquad \delta = (1 - \epsilon_p)X_p - \hat{X}_p \tag{4.35}$$

The channel coefficient seen by *Equalizer 2*, βh_{22}, is estimated from secondary pilots. Output of *Equalizer 2* is given by

$$Y_s = (1 - \epsilon_s)X_c + \frac{\delta}{\beta \hat{h}_{22}} + \frac{1}{\hat{h}_{22}} Z_s \tag{4.36}$$

where the channel estimation error, ϵ_s, for the secondary signal is

$$\epsilon_s = 1 - \frac{h_{22}}{\hat{h}_{22}} \tag{4.37}$$

Finally, the secondary signal estimate, $\hat{X}_c$, is obtained by quantizing the equalized signal to one of the constellation points in the modulation alphabet.

Chapter 5

Implementation

In this chapter practical implementations of overlay cognitive radios in two different OFDM based physical layers, WLAN-type (IEEE802.11g/n) and LTE-type, are presented. The systems are implemented on GNU Radio [11] platform discussed in section 5.1.1. This platform allows implementation of cognitive radios in software making it easily and dynamically reconfigurable.

5.1 Implementation platform

Cognitive radios are implemented by SDR (Software Defined Radio) technology. The main idea behind SDR is a move towards replacing functionalities of hardware components by software. Even though the degree to which parts of the radio are implemented by software programs varies, a SDR, in general, has two parts: software running on host machines and RF hardware attached to antenna as shown in Figure 5.1.

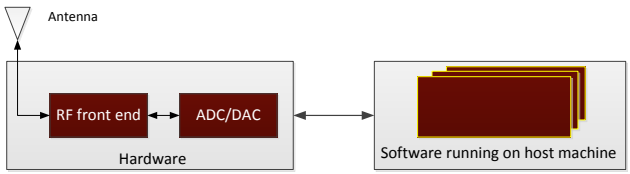

Figure 5.1: Software define radio.

5.1.1 GNU Radio and USRP

GNU Radio [11] is an open-source platform for developing SDRs. It has a set of signal processing libraries (called *blocks*) that are written in C++. Software radio applications are implemented by building a flow graph either in C++ or Python where nodes are signal processing blocks and branches represent the data stream. The software handles the baseband signal processing tasks related to the physical layer. Upper layer protocols can be implemented by creating necessary interfaces, usually known as *service access points* in networking technology terms.

The software is used with external hardware which is connected to the antenna and handles RF signal processing and ADC/DAC (Analog-to-Digital Conversion / Digital-to-Analog Conversion). The most common hardware platform used with GNU Radio is the the Universal Software Radio Peripheral (USRP) [33]. GNU Radio transmits/receives digital baseband data stream to/from the USRP using a Universal Hardware Driver (UHD) [34] through computer's USB (Universal Serial Bus) or Gigabit Ethernet interface.

The main functionalities of USRP are conversion between baseband and RF, filtering, analog to digital conversion (during reception), pulse shaping and digital to analog conversion (during transmission). The USRP has a motherboard containing FPGA (Field Programmable Gate Array) chip, ADC's and DAC's. The motherboard can be connected to various types of RF cards (*daughterboards*) that support different frequency bands such as GSM 900 and 1800, 2.4 GHz and 5 GHz ISM bands. Figure 5.2 shows interfaces of GNU radio with upper layers and the USRP hardware.

5.2 WLAN-type overlay transmitter

The WLAN-type overlay transmitter shown in Figure 5.3 implements the *orthogonal-pilot* scheme as presented in Section 4.3. Upper part of the transmitter is responsible for generation of relayed DVB signal. Inputs to the DVB transmitter are encoded message bytes. Secondary message is encoded and

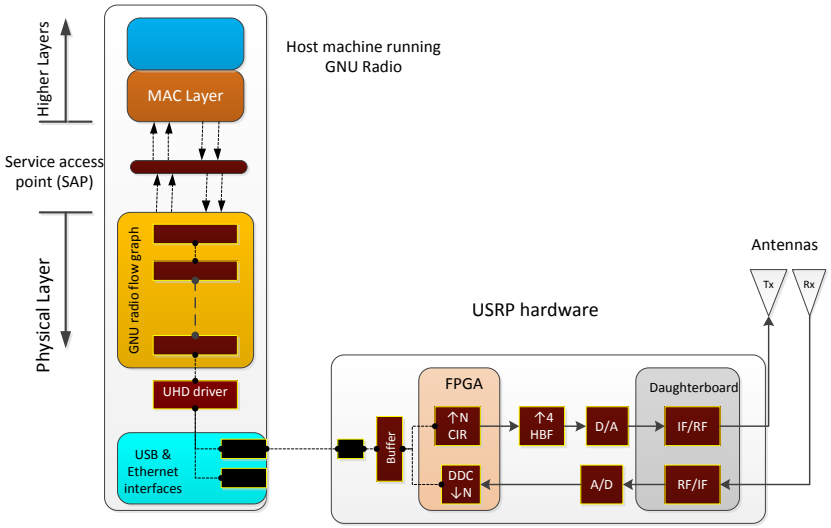

Figure 5.2: Interaction among USRP hardware, GNU Radio and upper layers.

mapped to carriers by the lower half of the transmitter. The transmitter's power is partly allocated for the primary signal at chosen proportion. After all stages of various signal processing, the physical layer sends complex base-band time-domain samples to the USRP.

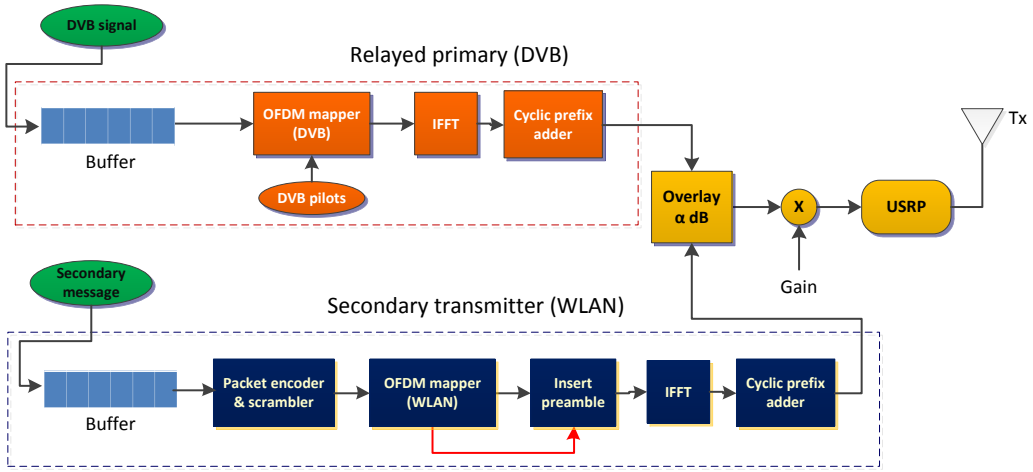

Figure 5.3: WLAN-type OFDM transmitter implementation using GNU Radio platform.

5.2.1 Packet encoder and scrambler

It receives packets (stream of bytes) from upper layer. The packet is then appends with CRC (Cyclic Redundancy Check) bits. The encoded packet is then scrambled with random sequence known to both the transmitter and the receiver. Packet header that contains information about scrambling and packet length is appended at beginning of the packet. Finally, encoded and scrambled bits are passed to the OFDM mapper.

5.2.2 OFDM mapper

Depending on type of modulation chosen, encoded sequence of bits is divided into groups of bits where each group corresponds to a constellation point in the modulation alphabet. Groups of bits are converted to modulated symbols (complex samples). Frequency-domain OFDM symbol is created as vector of complex samples. Zeros are padded on either sides of the vector as the FFT length is typically made to be larger than signal bandwidth. When N_U subcarriers are occupied in an OFDM symbol of length $N_{FFT} \geq N_U$, N_U modulated symbols are mapped to one OFDM symbol.

The DVB OFDM mapper assigns modulated symbols and reference pilot to sets of carriers according to the specification [1]. One OFDM symbol is produced per input packet. On the other hand, the number of OFDM symbols produced by WLAN OFDM mapper depends on the packet size and modulation. This mapper does not use carriers reserved for *continual pilots* of the DVB signal.

5.2.3 Insert preamble

The frame length in the WLAN-type physical layer varies according to the packet length. Each packet is transmitted independently, hence the receiver must be able to detect individual packets. Preambles are appended at the beginning of each packet to aid synchronization at the receiver.

5.2.4 IFFT

This block transforms frequency-domain OFDM symbol to time-domain counterpart through DFT (Discrete-time Fourier Transform).

5.2.5 Cyclic prefix adder

The cyclic prefix is added to avoid ISI (Inter-Symbol-Interference) caused by multipath propagation. A cyclic prefix of length n is added to each OFDM symbol by appending the last n samples to the beginning of the symbol.

5.2.6 Gain

Baseband samples are scaled by desired constant to control transmitted signal power.

5.2.7 USRP

The USRP is responsible for converting discrete samples into continuous analog signal and translating the baseband signal to transmission carrier frequency.

5.3 WLAN-type overlay receiver

Decoding of secondary message is a two-step process as shown in Figure 5.4. Since the primary signal is stronger than the secondary, the receiver decodes the primary message first. Then, the primary signal samples are reconstructed. These estimates are subtracted from received signal. The residual signal contains secondary signal, noise and interference from the primary caused by estimation error. The secondary message is then decoded from the residual signal in a similar fashion as done to decode the primary message.

5.3.1 USRP

The USRP transforms the signal of interest at a given carrier frequency into baseband signal.

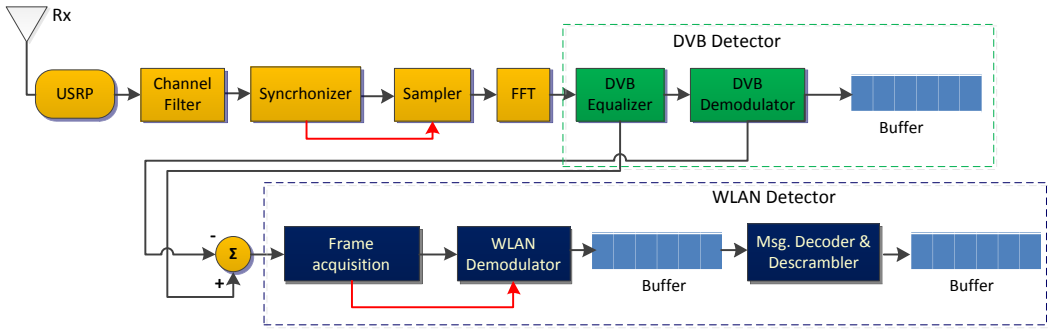

Figure 5.4: GNU Radio implementation of WLAN-type overlay receiver.

5.3.2 Channel filter

Since only a subset of subcarriers in the OFDM symbol are used, higher frequency part of received baseband signal from the USRP is eliminated by a low-pass channel filter before applying further signal processing.

5.3.3 Synchronizer

This is the fundamental part of the receiver. The receiver has to know transmission time instant of every packet. Every transmitted OFDM symbol is appended with cyclically extended samples. The receiver uses this information to apply autocorrelation for detection of symbols, and hence packets. Moreover, by estimating the phase offset between cyclic prefix samples, carrier frequency offset between transmitter and receiver is estimated. Only fractional part of the frequency offset less than subcarrier spacing can be detected by the synchronizer. Remaining, if any, part of the frequency offset which is in the order of integral multiple of subcarrier spacing is estimated by the DVB Equalizer block discussed in Section 5.3.6. The synchronizer has internal numerically-controlled oscillator that compensates for the fractional frequency offset.

5.3.4 Sampler

The sampler picks one OFDM symbol (a vector of length equal to FFT length) from stream of samples at a time. Timing information is received from the synchronizer. Cyclic prefix samples are removed at this stage. Under per-

fect synchronization, OFDM samples can be obtained by removing the first n (cyclic prefix length) samples leaving next N samples corresponding to an OFDM symbol. However, if the symbol timing shifted even by one sample into the symbol, ISI occurs. Therefore, the sampler is designed to be flexible in such a way that it can be configured to start sampling at the middle (or any other position) of the cyclic prefix. The sampler automatically cyclically shifts the samples in order to avoid carrier phase rotation.

5.3.5 FFT

This block performs standard DFT (Discrete-time Fourier Transform) on each OFDM symbol.

5.3.6 DVB equalizer

This block is responsible for IFO (Integer Frequency Offset) compensation and channel equalization. IFO, if any, is detected by correlating received signal with pre-generated *continual pilot* symbols. Then phase rotation due to sampling offset is compensated. Finally, the received symbols are equalized by channel estimates using pilot signals.

5.3.7 DVB demodulator

Equalized complex symbols are quantized to constellation points in the modulation alphabet used by the DVB transmitter. Then packets formed from demodulated symbols are passed to the upper layer via output buffer. The demodulator also outputs residual signal (after quantized symbols are subtracted from received signal) to the second stage of decoding.

5.3.8 Frame acquisition

This block basically performs two task. First, it detects the preambles by correlating each OFDM symbol with pre-generated preamble sequence. Second, it estimates the channel from preambles and equalizes OFDM symbols of a packet following the preamble.

5.3.9 WLAN demodulator

Complex secondary symbols are demodulated into bits. Packet length and information about scrambling are extracted from the first set of bits that belong to the packet header. The demodulator accumulates as many bytes as the encoded packet length and passes them to the decoder.

5.3.10 Message decoder and descrambler

Received byte streams are descrambled and decoded. Decoded message and CRC test (whether the packet is correctly received or not) are passed to the upper layer via a message queue.

5.4 LTE-type overlay transmitter

The LTE physical layer was implemented based on specifications in [16] and [35]. These specifications define transmitter characteristics only. There is no unique algorithm for receiver implementation rather it is vendor specific even though one can understand the basic requirements for the receiver to reliably communicate with the transmitter. In our receiver implementation, we will use most commonly known algorithms.

The LTE overlay transmitter operation is similar to that of WLAN-type physical layer discussed in Section 5.2. Figure 5.5 shown the implementation architecture. The secondary transmitter (LTE) contains layer mapping and precoding functionalities for MIMO (Multiple Input Multiple Output) applications. Since the overlay system assumes SISO (Single Input Single Output) configuration, the two blocks can be bypassed. Since single antenna port is used, no diversity and multiplexing functions are needed. Resource blocks can be scheduled every subframe though lengths of transmitted codewords on LTE transmitter can span multiple subframes provided that packet length is known by the receiver.

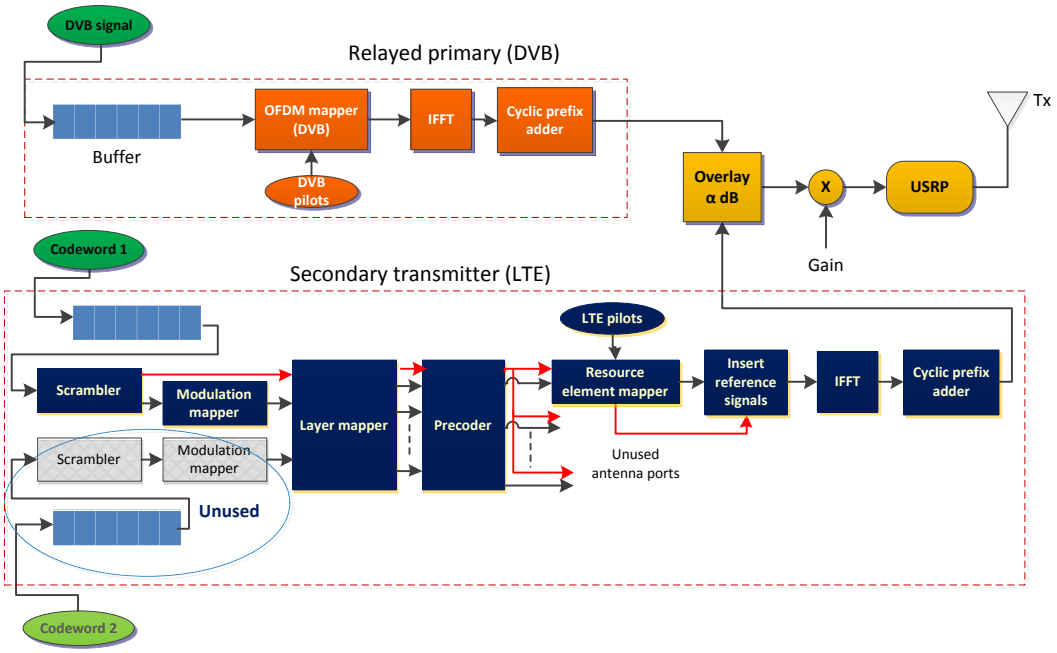

Figure 5.5: GNU Radio implementation of LTE DL overlay transmitter.

5.4.1 Scrambler

Input codeword bits are scrambled by a random sequence generated in systematic way. The receiver extracts scrambling information during initial synchronization. Outputs of the scrambler are packed bits. n bits are packed into one symbol when the modulation has 2^n alphabets.

5.4.2 Modulation mapper

This block maps each packet bit (symbol) into a constellation point (complex number) in the modulation alphabet.

5.4.3 Layer mapper

This block operates in conjunction with the precoder. It takes one or two streams of complex symbols where each stream corresponds on a codeword, and then maps them into one or more layers. The number of layers is determined by number of codewords and type of antenna configuration: single antenna port (default), transmit diversity, or spatial multiplexing. In single antenna

port configuration, the layer mapper directly maps its inputs to the output port.

5.4.4 Precoder

This block is responsible for encoding of layers by codewords specified for LTE Downlink transmission [16]. Outputs of the precoder are m parallel streams where m is the number of antenna ports.

5.4.5 Resource element mapper

In LTE resources are divided into resource blocks. A resource block corresponds to 12 subcarriers used over one time slot. A single subcarriers is called resource element. Resource blocks are scheduled dynamically so that different sets of resource elements can be used for transmission at different instances of time. The *resource element mapper* block maps precoded symbol on subcarriers belonging to scheduled resource blocks. Pilot symbols that aid channel estimation are also inserted at known locations in each resource block. One frequency-domain OFDM symbol is produced as output at a time.

5.4.6 Insert reference signals

This block inserts primary and secondary synchronization sequences in every frame. Unlike the WLAN-type physical layer, LTE frame is divided in fixed time slots and synchronization signal are transmitted at constant interval of time.

5.4.7 IFFT

It performs IDFT to each OFDM symbol.

Cyclic prefix adder

It adds cyclic prefix to each OFDM symbol. Normal cyclic prefix configuration defined in [16] is used.

5.4.8 USRP

Stream of complex baseband samples are converted into continuous analog waveform and transmitted at a given carrier frequency.

5.5 LTE overlay receiver

The receiver shares the same DVB detector as WLAN-type receiver discussed in Section 5.3. Sequential decoding of the secondary message is also done in a similar fashion. The LTE detector uses only on antenna port as shown in Figure 5.6. .

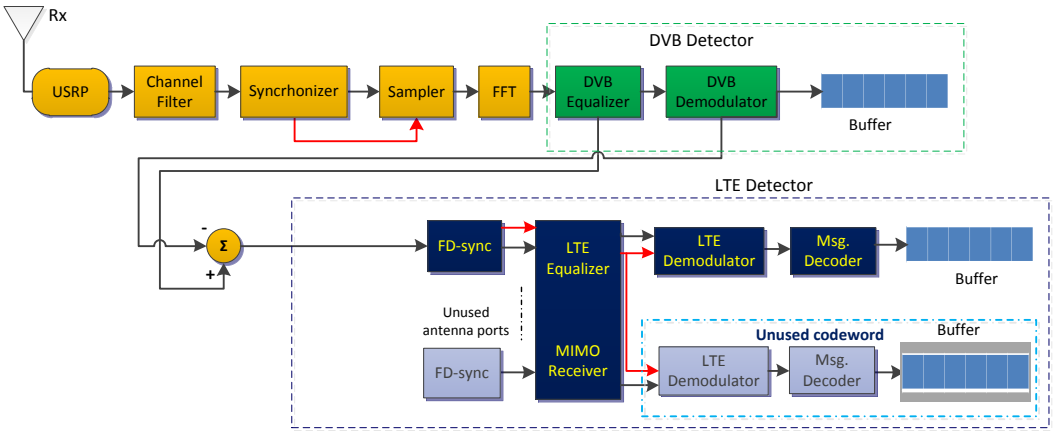

Figure 5.6: GNU Radio implementation of LTE-type overlay receiver.

5.5.1 FD-sync

In LTE there 504 unique cell-identities which are grouped into 168 groups each containing 3 cell identities [16]. The first synchronization sequence identifies one cell identity in a group. The second synchronization sequence is generated by parameters which are unique to a physical cell identity group. Hence a cell (and hence its associated parameters) can be identified among 504 cells. The FD-sync block performs frequency-domain synchronization. By correlating received synchronization symbols with pre-generated primary and secondary synchronization sequences.

5.5.2 Equalizer

Cell-specific and UE-specific reference signals are interleaved in time and frequency with data symbols. The equalizer tracks channel variation using these pilot signals. When multiple antenna ports are used, diversity combining or MIMO reception algorithms can be used. In this overlay transmission, these features are not used as a single antenna port is assumed in transmission.

5.5.3 LTE demodulator

Complex symbols transmitted on scheduled resource blocks are demodulated into bits. The demodulator descrambles every demodulated bit on the fly. Packet length information is extracted from the first set of bits that belong to the packet header. The demodulator accumulates as many bytes as the encoded packet length and passes them to the decoder. In the default configuration, the demodulator assumes that a packet fits within a subframe. On the other hand, if the packet length is explicitly defined, a packet can span multiple subframes. The block can be dynamically reconfigured in every subframe when new set of resource blocks are assigned to the user.

5.5.4 Message decoder

Received packets are decoded and passed to the upper layer together with CRC test result (whether the packet is correctly received or not) via a message queue.

Chapter 6

Results and Discussion

This chapter discusses performance measurement results of physical layer implementations of the two overlay cognitive radio schemes whose implementation was presented in the previous chapter. BER (Bit-Error-Rate) of primary and secondary transmissions in different SNR levels are shown for a set of modulation types.

6.1 Hardware characteristics

As described in previous chapter, the USRP hardware is used as RF front-end. This device supports a variety of daughterboards which should be mounted on its motherboard. Daugherboards are responsible for the final RF tuning of signals transmitted/received to/from the antenna. Different daughterboards support different range of frequencies. Table 6.1 shows characteristics of specific hardware components used in the measurement.

6.2 Measurement setup

Due to spectrum license issues, the system was tested in the ISM-band at 2.4 GHz carrier frequency. CRC bits are appended to every transmitted packet, and no error-correcting channel codes are used. The receiver computes the BER by comparing received bit stream with local copy of transmitted mes-

USRP Box	Model	USRP N200
	Input channel	1 I-Q pair
	Output channel	1 I-Q pair
	Sample rate	100M Samples/s
	Input resolution	14 bits
	Output resolution	16 bits
	SFDR[1]	80+ dB
	Maximum bandwidth	25 MHz
Daughterboard	Model	SBX
	Frequency range	400 MHz - 4.4 GHz
	Transmit power	30 - 100 mW typical
	Noise Figure	6-8 dB

Table 6.1: RF characteristics of hardware used during measurement.

sage. To avoid processing overhead on the host machine, a "2K mode" DVB signal was transmitted at nearly 2 MHz bandwidth (with sample rate of 2.083 MSamples/second).

In normal operation, the primary message would be transmitted by both the primary and the secondary transmitters where the later transmits its own message signal in addition to the relayed primary signal. To simplify measurements, either of primary and secondary signals were transmitted from only one transmitter. This corresponds to the case where the primary signal power relayed by the secondary transmitter is either very weak or very strong compared to the primary transmitter's power.

One way to control the SNR is to vary the transmission power through amplifier gain of the USRP. However, due to non-linearity of the RF front-end and in order to use full range of the DAC, the transmission power was kept constant. A controlled complex Gaussian noise was injected to the primary signal before it reaches the transmission antenna. Variance of the added noise was used to compute SNR. The computed SNR is upper limit of the received SNR as the former does not account for receiver's thermal noise. Since the signal power is made relatively high, effect of receiver's noise is negligible compared to the added noise at the transmitter. This is true especially in low SNR values.

Received signal at the secondary receiver is expressed as

$$Y = h_{12}\left(X_1 + Z_T\right) + h_{22}X_2 + Z_2 \tag{6.1}$$

where X_1 is the primary signal, X_2 is the secondary signal, Z_T is added noise, Z_2 is receiver's thermal noise, and $h_{i2},\ i \in \{1,2\}$ is channel gain from transmitter i to the secondary receiver. Assuming $E\{|Z_2|^2\} << E\{|h_{12}Z_T|^2\}$, primary and secondary SNR values are given by

$$SNR_1 \approx \frac{E\{X_1^2\}}{E\{Z_T^2\}} = \frac{P_1}{N_T} \tag{6.2}$$

$$SNR_2 \approx \frac{|h_{22}|^2 E\{X_2^2\}}{|h_{12}|^2 E\{Z_T^2\}} = \frac{|h_{22}|^2 P_2}{|h_{12}|^2 N_T} \tag{6.3}$$

where P_1 is transmitted primary signal power, P_2 is secondary signal power, and N_T is added noise power. We defined γ_p as ratio of the primary and secondary SNR's, or SIR (Signal-to-Interference Ratio) with respect to primary signal.

$$\gamma_p = \frac{SNR_1}{SNR_2} \tag{6.4}$$

In the following section, we will discuss BER measurement results for different values of γ_p.

6.3 Results

Figure 6.1 shows BER's of primary and secondary signals when powers of the two signals are comparable, i.e. $\gamma_p = 7dB$. It can bee seen that primary system's performance has not been degraded due to secondary transmissions on its pilot carriers when it is compared to the performance in *orthogonal-pilot* overlay transmission. This is due to the fact that the receiver's equalizer is able to filter the interference in long channel-tracking time window. However, there is SNR loss in both schemes compared to the theoretical performance.

The secondary signal's BER in *orthogonal-pilot* scheme is sufficiently close to the theoretical performance except that it has been bounded by the primary signals BER especially at higher SNR. On the other hand, *non-orthogonal pilot* transmission has severely degraded the secondary signal's performance.

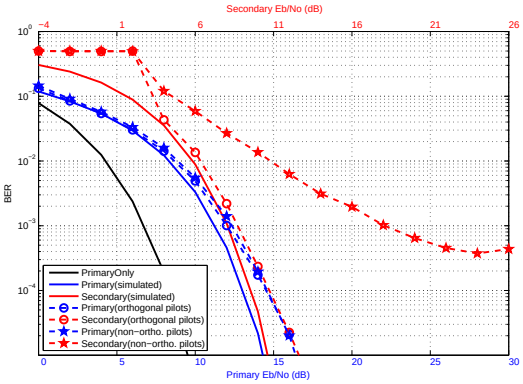

(a) Primary: 4QAM, Secondary: BPSK

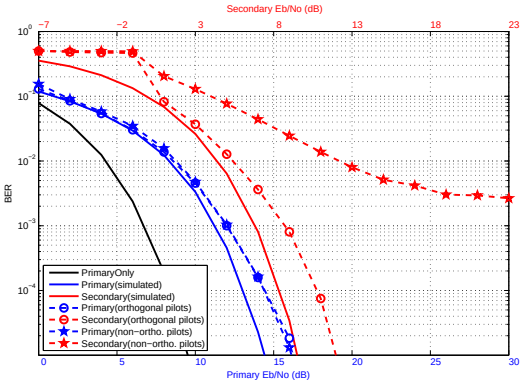

(b) Primary: 4QAM, Secondary: 4QAM

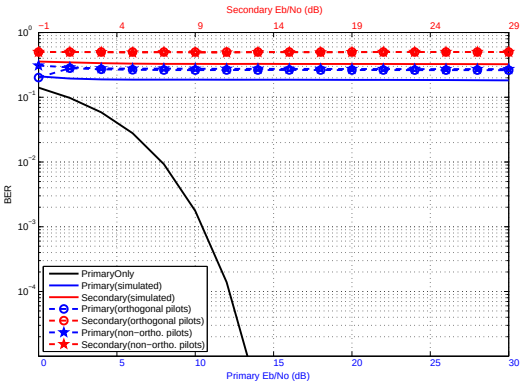

(c) Primary: 16QAM, Secondary: BPSK

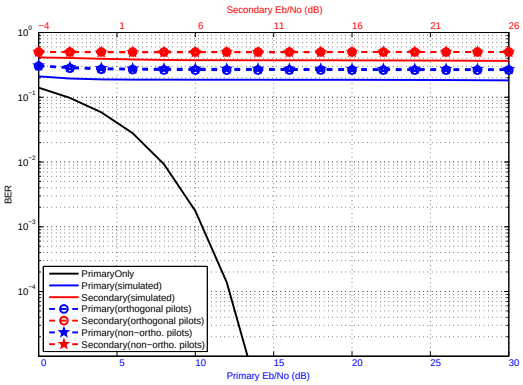

(d) Primary 16QAM, Secondary: 4QAM

Figure 6.1: Measured BER for primary and secondary signals, $\gamma_p = 7dB$.

In both schemes, all the secondary transmitter's messages were almost lost in low SNR regions (when secondary $E_b/N_o < 0$). The main reason is that the receiver was not able to detect the secondary transmitters synchronization pilots as the noise power is higher than the signal power. BER of secondary signal in *non-orthogonal pilot* overlay transmission seems to saturate at higher SNR values, i.e. when the added noise power is very small. This is because the receiver's internal noise outweighs the added noise so that the received SNR starts to divert from the computed value.

Figures 6.1c and 6.1d indicate that the primary message cannot be decoded when the secondary signal power is strong such that the signal constellations overlap. Therefore, in higher modulation schemes, where euclidean distance between constellation points is smaller, the secondary signal's power has to be reduced accordingly. As can bee seen from Figures 6.2c and 6.2d, higher γ_p value gives better performance. On can observe that reducing secondary signal power relative to the primary signal (increasing γ_p) also improves the secondary receiver's performance. This gain is more apparent in Figures 6.3c and 6.3d where $\gamma_p = 17dB$.

Figure 6.2 shows BER of primary and secondary signals when $\gamma_p = 12dB$. Since the secondary signal power is weaker compared to the case when $\gamma_p = 7dB$ (shown in Figure 6.1), the primary signal BER falls below 10^{-5} at relatively lower SNR where effect of receiver's noise is small. Therefore, measured BER is seen to be very close to the theoretical value. This has also been observed in Figure 6.3 where $\gamma_p = 17dB$. However, domination of receiver's noise is reflected on the secondary receiver's performance at low added noise power (high computed primary SNR) since the secondary signal power is also quite low such that secondary SNR is much less than primary SNR.

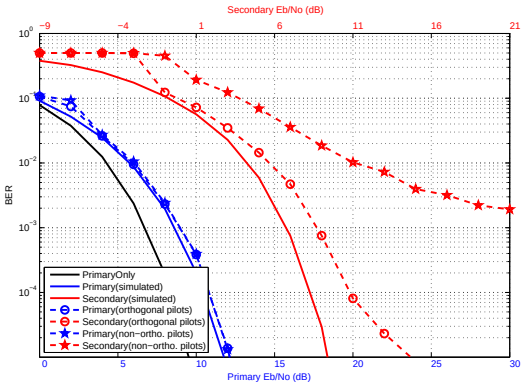

(a) Primary: 4QAM, Secondary: BPSK

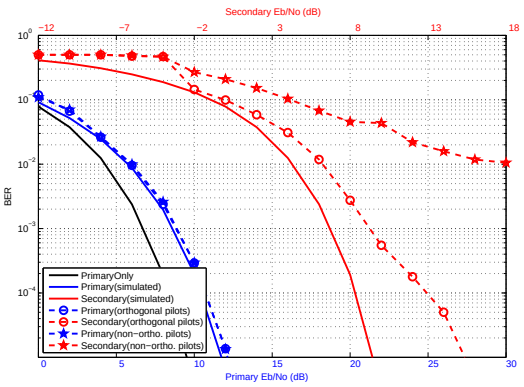

(b) Primary: 4QAM, Secondary: 4QAM

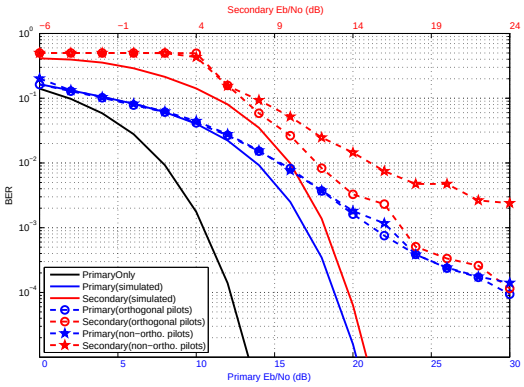

(c) Primary: 16QAM, Secondary: BPSK

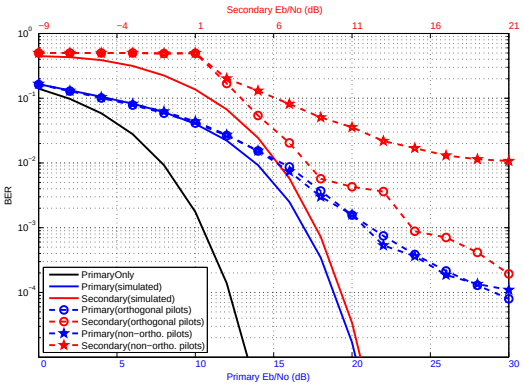

(d) Primary 16QAM, Secondary: 4QAM

Figure 6.2: Measured BER for primary and secondary signals, $\gamma_p = 12dB$.

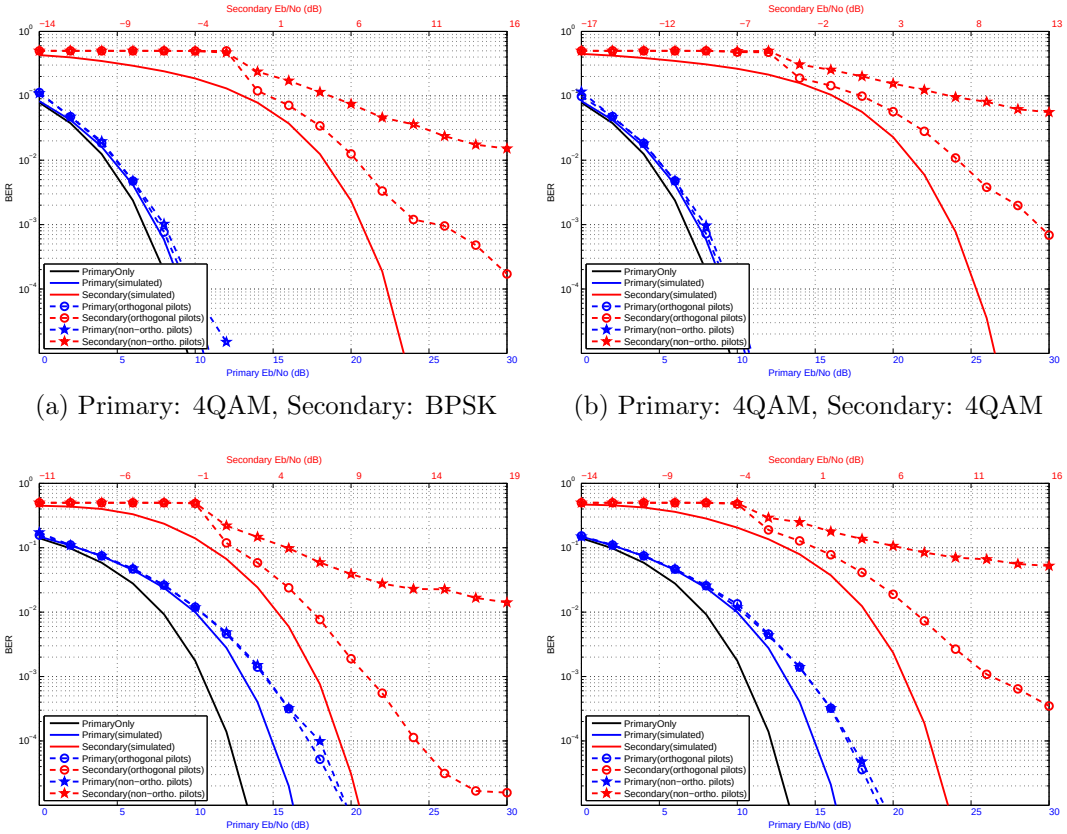

(a) Primary: 4QAM, Secondary: BPSK

(b) Primary: 4QAM, Secondary: 4QAM

(c) Primary: 16QAM, Secondary: BPSK

(d) Primary 16QAM, Secondary: 4QAM

Figure 6.3: Measured BER for primary and secondary signals, $\gamma_p = 17dB$.

Chapter 7

Conclusion

With ever growing demand for wireless traffic, it is of great interest to have more efficient utilization of the limited radio resource. In improving spectral efficiency of data transmission in fading environments, OFDMA is the leading modulation scheme used in current technologies. Diversity combining and spatial multiplexing via multiple antennas have also been used to exploit multipath channels.

While there have been developments in maximizing efficiency of a specific radio access technology that operates on a specific frequency band, capacity loss due to brick wall type of allocation of the spectrum to licensed users had got less attention. Non-orthogonal access to a shared resource has been found to achieve higher capacity. A spectrum that is primarily granted to a licensed user is shared by other secondary systems through complex schemes that guarantee tolerable interference to the primary system.

Cognitive radio is a promising technology to enable such flexible spectrum usage by multiple users. The TV band has been the target spectrum for secondary spectrum access. The secondary systems may use the resource when it is free. On the other hand, a more complex technique is to overlay secondary signal on the primary signal at relatively low power, and apply interference mitigation at the receiver. This *overlay cognitive radio* was studied in this thesis.

A *black-space spectrum* using overlay cognitive radios has been tested to be realizable on software defined radios. Even though theoretical achievable capacity limits of this technique have been studied in many literatures [8], [7], [12], [13], this thesis addresses practical realization of secondary systems, and their performances in real channel environments. According to pilot structures of targeted secondary systems, WLAN and LTE, we can have two types of cognitive radios, *orthogonal pilot* and *non-orthogonal pilot*.

Results have shown that under certain constraints, both primary and secondary systems effectively communicate simultaneously over a shared channel. The main constraint is that the secondary transmitter's power should be much less than primary transmitter's power. This interference level is determined by modulation type used in the primary signal. Higher order primary modulation requires the secondary to transmit at even lower power. In some cases reducing secondary transmitter's power benefits both the primary and the secondary systems.

We have also seen that secondary transmission on primary pilot carriers does not affect the primary system's performance much when it is compared to transmissions which are orthogonal to pilot carriers. However, secondary system's performance severely degraded.

Bibliography

[1] EN 300 744 V1.6.1, "European Standard (Telecommunications series) Digital Video Broadcasting (DVB); Framing structure, channel coding and modulation for digital terrestrial television," STSI, Tech. Rep., 2009.

[2] "IEEE standard for information technology-telecommunications and information exchange between systems-local and metropolitan area networks-specific requirements - part 11: Wireless lan medium access control (mac) and physical layer (PHY) specifications," pp. C1 –1184, 2007.

[3] M. Pun, M. Morelli, and C.-C. J. Kuo, *Multi-Carrier Techniques for Broadband Wireless Communications: a Signal Processing Perspective*. Imperial College Press, 2007.

[4] "Report of the spectrum policy task force, ET docket no. 02-135," Federal Communications Commission, Tech. Rep., Nov. 2002.

[5] J. Mitola, "Cognitive radio: An integrated agent architecture for software defined radio," PhD Thesis, Royal Institute of Technology (KTH), Teleinformatics, 2000.

[6] "Definitions of Software Defined Radio (SDR) and Cogntive Radio Systems (CRS)," ITU-R SM.2152, Tech. Rep., Sept. 2009.

[7] S. Haykin, "Cognitive radio: brain-empowered wireless communications," *Selected Areas in Communications, IEEE Journal on*, vol. 23, no. 2, pp. 201 – 220, feb. 2005.

[8] A. Goldsmith, S. Jafar, I. Maric, and S. Srinivasa, "Breaking spectrum gridlock with cognitive radios: An information theoretic perspective," *Proceedings of the IEEE*, vol. 97, no. 5, pp. 894 –914, may 2009.

[9] N. Alonistioti, S. Panagiotakis, M. Koutsopoulou, V. Gazis, and N. Houssos, *Software Defined Radio: Architectures, Systems and Functions*. John Wiley & Sons, 2003, pp. 165–189.

[10] *Cognitive Radio, Software Defined Radio, and Adaptive Wireless Systems (Signals and Communication Technology)*. Springer, Sep. 2007.

[11] (2011, December 25) Gnu radio home page. [Online]. Available: http://gnuradio.org/redmine/projects/gnuradio/wiki

[12] A. Jovicic and P. Viswanath, "Cognitive radio: An information-theoretic perspective," in *Information Theory, 2006 IEEE International Symposium on*, july 2006, pp. 2413 –2417.

[13] N. Devroye, P. Mitran, and V. Tarokh, "Achievable rates in cognitive radio channels," *Information Theory, IEEE Transactions on*, vol. 52, no. 5, pp. 1813 – 1827, may 2006.

[14] L. Geoffrey and L. Gordon, *Orthogonal Frequency Division Multiplexing for Wireless Communications*. Springer Science+Business Media Inc., 2006.

[15] "ETSI TR 125 943 v8.0.0 - Universal Mobile Telecommunications System (UMTS); deployment aspects (3GPP TR 25.943 version 8.0.0 release 8)," Tech. Rep., 2009.

[16] "3GPP TS 36.211 v8.9.0 - 3^{rd} Generation Partnership Project; Technical Specification Group Radio Access Network; Evolved Universal Terrestrial Radio Access (E-UTRA); physical channels and modulation (Release 8)," Tech. Rep., 2009.

[17] "IEEE standard for information technology- telecommunications and information exchange between systems-local and metropolitan area

networks-specific requirements-part 11: Wireless lan medium access control (mac) and physical layer (PHY) specifications," pp. i –445, 1997.

[18] H.-S. Chen, W. Gao, and D. Daut, "Spectrum sensing using cyclostationary properties and application to ieee 802.22 wran," in *Global Telecommunications Conference, 2007. GLOBECOM '07. IEEE*, nov. 2007, pp. 3133 –3138.

[19] Z. Ye, J. Grosspietsch, and G. Memik, "Spectrum sensing using cyclostationary spectrum density for cognitive radios," in *Signal Processing Systems, 2007 IEEE Workshop on*, oct. 2007, pp. 1 –6.

[20] S. Shellhammer, A. Sadek, and W. Zhang, "Technical challenges for cognitive radio in the tv white space spectrum," in *Information Theory and Applications Workshop, 2009*, feb. 2009, pp. 323 –333.

[21] M. Nekovee, "Cognitive radio access to tv white spaces: Spectrum opportunities, commercial applications and remaining technology challenges," in *New Frontiers in Dynamic Spectrum, 2010 IEEE Symposium on*, april 2010, pp. 1 –10.

[22] S. Shellhammer, "A comparison of geo-location and spectrum sensing in cognitive radio," in *Computer Communications and Networks, 2009. ICCCN 2009. Proceedings of 18th International Conference on*, aug. 2009, pp. 1 –6.

[23] C. Luo, F. Yu, and H. Ji, "Optimal capacity in underlay paradigm based cognitive radio network with cooperative transmission," in *Vehicular Technology Conference Fall (VTC 2010-Fall), 2010 IEEE 72nd*, sept. 2010, pp. 1 –5.

[24] K. Son, B. C. Jung, S. Chong, and D. K. Sung, "Opportunistic underlay transmission in multi-carrier cognitive radio systems," in *Wireless Communications and Networking Conference, 2009. WCNC 2009. IEEE*, april 2009, pp. 1 –6.

[25] A. Carleial, "Interference channels," *Information Theory, IEEE Transactions on*, vol. 24, no. 1, pp. 60 – 70, jan 1978.

[26] T. Han and K. Kobayashi, "A new achievable rate region for the interference channel," *Information Theory, IEEE Transactions on*, vol. 27, no. 1, pp. 49 – 60, jan 1981.

[27] H. Weingarten, Y. Steinberg, and S. Shamai, "The capacity region of the gaussian mimo broadcast channel," in *Information Theory, 2004. ISIT 2004. Proceedings. International Symposium on*, june-2 july 2004, p. 174.

[28] M. Costa, "Writing on dirty paper (corresp.)," *Information Theory, IEEE Transactions on*, vol. 29, no. 3, pp. 439 – 441, may 1983.

[29] U. Erez and S. Brink, "A close-to-capacity dirty paper coding scheme," *Information Theory, IEEE Transactions on*, vol. 51, no. 10, pp. 3417 – 3432, oct. 2005.

[30] U. Erez, S. Shamai, and R. Zamir, "Capacity and lattice strategies for canceling known interference," *Information Theory, IEEE Transactions on*, vol. 51, no. 11, pp. 3820 – 3833, nov. 2005.

[31] C. E. Shannon, "Channels with side information at the transmitter," *IBM J. Res. Dev.*, vol. 2, pp. 289–293, October 1958. [Online]. Available: http://dx.doi.org/10.1147/rd.24.0289

[32] F. M. J. Willems, "On gaussian channels with side information at the transmitter," in *Proc. 9th Symp. Information Theory in the Benelux, Enschede, The Netherlands*, april 1988.

[33] (2011, December 25) Ettus research llc. [Online]. Available: http://ettus.com/products

[34] (2011, December 25) Universal hardware driver. [Online]. Available: http://code.ettus.com/redmine/ettus/projects/uhd/wiki

[35] "3GPP ts 36.213 v8.8.0 - 3^{rd} Generation Partnership Project; Technical Specification Group Radio Access Network; Evolved Universal Terrestrial Radio Access (E-UTRA); physical layer procedures (Release 8)," Tech. Rep., 2009.